

DESIGN OF AN AXIAL FLOW BIOREACTOR FOR  
TISSUE REGENERATION

By

PRASANA RAJA BHASKAR

Bachelor of Engineering in Chemical Engineering

Master of Science in Chemistry

BITS-PILANI

Goa, India

2009

Submitted to the Faculty of the  
Graduate College of the  
Oklahoma State University  
in partial fulfillment of  
the requirements for  
the Degree of  
MASTER OF SCIENCE  
May, 2012

DESIGN OF AN AXIAL FLOW BIOREACTOR FOR  
TISSUE REGENERATION

Thesis Approved:

Dr. Sundar V. Madihally

---

Thesis Adviser

Dr. Heather Fahlenkamp

---

Dr. AJ Johannes

---

Dr. Sheryl A. Tucker

---

Dean of the Graduate College

## TABLE OF CONTENTS

Chapter	Page
I. INTRODUCTION .....	1
II. BACKGROUND.....	5
2.1 Tissue Engineering.....	5
2.2 Porous Scaffolds .....	7
2.3 Bioreactors in Tissue Engineering .....	9
2.4 Computational Fluid Dynamics Simulation.....	15
2.5 Fluid Flow Characteristics .....	17
2.6 Nutrient Distribution with Consumption .....	18
2.7 Importance of Residence Time Distribution.....	20
III. OPTIMIZATION OF BIOREACTOR VIA CFD SIMULATION .....	22
3.1 Introduction.....	22
3.2 Setting the Simulation.....	23
3.2.1 Creating the Bioreactor Design.....	23
3.2.2 Selection of Governing Equations and the Boundary Conditions .....	24
3.2.2.1 Fluid Flow Characteristics .....	25
3.2.2.2 Nutrient Consumption Pattern .....	26
3.2.3 Meshing the System.....	28
3.2.4 Generating Results .....	28
3.3 Results.....	28
3.3.1 Effect of Increased Scaffold Diameter.....	28
3.3.2 Influence of Semi Angle on Nutrient Distribution .....	32
3.3.3 Incorporating a Distribution System .....	34
3.3.4 Effect of Changes in Inlet and Outlet Diameters .....	36
3.3.5 Influence of Scaffold Thickness .....	39
3.3.6 Effect of Flow Rate.....	41
3.3.7 Effect of Permeability on Pressure Drop .....	43
3.4 Summary .....	45

Chapter	Page
IV. EXPERIMENTAL VALIDATION.....	46
4.1 Introduction.....	46
4.2 Materials and Methods.....	47
4.2.1 Bioreactor Construction .....	47
4.2.2 Preparation of the Porous Scaffold .....	47
4.2.3 Validating Pressure Drop .....	48
4.2.4 Residence Time Distribution Analysis .....	51
4.3 Results and Discussion .....	54
4.3.1 Pressure Drop Comparison .....	54
4.3.2 Residence Time Distribution .....	55
V. CONCLUSION AND RECOMMENDATIONS.....	61
5.1 Conclusion .....	61
5.2 Recommendations.....	63
REFERENCES .....	64
APPENDICES .....	68
A. COMSOL 4.2 Manual.....	68
B. Experimental Observations.....	85

## LIST OF TABLES

Table	Page
1. Pore Architecture .....	26
2. Rate Constants for Smooth Muscle Cells .....	27
3. Values of the Number of Cells and $V_M$ .....	29
4. Effect of Increased Scaffold Diameter.....	31
5. Influence of Semi Angle on Nutrient Distribution .....	33
6. Effect of Inlet Diameter on Pressure Drop and Nutrient Concentration.....	37
7. Effect of Outlet Diameter on Pressure Drop and Nutrient Concentration .....	38
8. Effect of Scaffold Thickness on Pressure Drop and Nutrient Concentration .....	40
9. Effect of Flow Rate on Pressure Drop and Nutrient Concentration .....	42
10. Effect of Pore Size on Permeability.....	43
11. Effect of Permeability on Pressure Drop .....	44
12. Comparison of Residence Time Distributions .....	60

## LIST OF FIGURES

Figure	Page
1. Basic Principle of Tissue Engineering .....	6
2. Types of High Aspect Ratios .....	13
3. Axial Flow Bioreactors in Use .....	14
4. Steps Involved in CFD Simulation .....	23
5. Effect of Bioreactor Design on Nutrient distribution .....	35
6. Constructed Bioreactor Pieces .....	47
7. Schematic of the CRFLT Process used in Scaffold Generation .....	48
8. Experimental Setup to Measure Pressure drop Across the Bioreactor .....	50
9. Schematic of the Perfusion System to Assess the Residence Time Distribution in the Bioreactor .....	51
10. Experimental Validation of Pressure drop (Pa) vs. Flow Rate (mL/min).....	55
11. Transient Changes in the Concentration of the Tracer at the Outlet of the Axial Flow Bioreactor .....	57
12. E-Curve for the Axial Flow Bioreactor .....	58
13. tE(t) vs t Curve.....	59

## CHAPTER I

### INTRODUCTION

Patients suffering from organ failure need engineered tissues when there is a scarcity of matched sources. Engineered tissues which can be implanted into the recipient provide an alternative to traditional organ donation. In tissue engineering, cells are seeded on to porous scaffolds generated from biodegradable materials. Cells are populated and matured into tissues by supplying nutrients in bioreactors that facilitate uniform distribution. A bioreactor is an essential component for culture of cells in vitro for i) providing the way of mechanical stimulation of cells essential for certain cell growth through the flow of nutrient medium and ii) maintaining uniform pH and temperature. There are many configurations of bioreactors based on the type of mixing and flow scheme. Particularly, the axial flow bioreactors are of interest to regenerate a variety of tissues as they offer several advantages, such as convection-driven nutrient distribution and the ability to operate at high flow rates. The flow is axial when the inlet, scaffold and outlets are oriented along the same axis. Currently used axial flow bioreactors have different dimensions and have been used for tissue culture of many types of cells.

Many of the dimensions in the bioreactor generation are randomly selected without a rational basis. No systematic modeling to study the hydrodynamic characteristics and nutrient distribution has been performed.

Modeling the bioreactors using the Computational Fluid Dynamics (CFD) simulation tools has been adapted for other types of bioreactors, such as flow-through, parallel-flow and rotary. Modeling was done mainly to study the hydrodynamic characteristics, such as the shear stress and the pressure drop, and the nutrient distribution. This type of modeling has to be extended to the axial flow bioreactor. Different geometric dimensions are to be optimized in the bioreactor to ensure uniform shear stress and nutrient distribution throughout the region of scaffold. Experimental validation of modeling through simulation is necessary to prove the credibility of simulation. Hence the specific aims of this study are:

### **Specific Aim 1: Optimization of Bioreactor via CFD Simulation**

Bioreactor design has several parameters such as the inlet or outlet diameters, or the scaffold thickness that require optimization. In addition, different cells need different factors suitable for their growth, including the flow rate, shear stress, and nutrient consumption. As a part of optimizing the design of the axial flow bioreactor, the effect of scaling up was analyzed, showing uniform distribution in all reactors. The diameter of the bioreactor was first scaled up from  $x$  mm to  $5x$  mm to accommodate corresponding size scaffolds without altering the thickness and geometric shape of the bioreactor. The initial bioreactor had an angular entry to facilitate uniform distribution of nutrients. Since the scaled up bioreactor had large hold-up volume, the semi-angle ( $sa^\circ$ ) of the entry cone



was increased from  $sa^\circ$  to  $2.67X\ sa^\circ$  to minimize the expensive medium hold-up volume. The increase in the semi-angle resulted in poor distribution of nutrients near the ends of the scaffold. Hence, incorporating a distributor system was considered in the entry region. Different configurations such as distributors and concentric baffles were evaluated. As the nutrient distribution of the newly designed bioreactor was satisfactory, further analysis was carried using this design to optimize several other factors. The inlet diameter was increased from  $id$  to  $3\ id\ mm$  and the outlet diameter was increased from  $od$  to  $3\ od\ mm$ . The thickness of the scaffold was increased from  $z\ mm$  to  $3\ z\ mm$  to determine the possibility of increasing the cell number in the bioreactor. The flow rate of the nutrient medium was increased from  $5\ mL/min$  to  $25\ mL/min$  to study the pressure drop across the bioreactor and the shear stress experienced by the cells. The permeability of the scaffold changes as the cell grows, and this effect was taken into account by decreasing the pore diameter from  $75\ \mu m$  to  $25\ \mu m$ . Based on these factors, an optimum bioreactor configuration was selected.

### **Specific Aim 2: Validation of the Simulation Results**

To validate the modeling approach and effectiveness of the newly designed axial flow bioreactor, experiments were conducted. Bioreactors were constructed according to the dimensions from specific aim 1. The pressure drop across the bioreactor was measured for the same flow rates as for the simulation. Experiments were conducted for the bioreactor with the scaffold and without the scaffold to validate the model of the bioreactor both in the non-porous and the porous region. A residence time distribution (RTD) analysis was carried out to understand the effect of the distributor system on the

nutrient distribution. The step input technique, which employs an injection of a red colored food dye, was used to obtain the RTD. RTD analysis was done for the bioreactor at a nutrient flow rate of 15 mL/min with the following conditions: a) without the distributor and without the scaffold, b) with the distributor and without the scaffold and c) with the distributor and with the scaffold. Theoretical mean residence time ( $t_m$ ) was calculated from the volumetric flow rate and the volume of the bioreactor. These calculations showed a dead volume of nearly 20% in the new bioreactor. These regions are similar to those observed in the simulation results.

Based on these analyses, various modifications are suggested which would significantly improve the performance of the bioreactor. These results show the possibility of using axial flow bioreactors for various tissue engineering applications.

## CHAPTER II

### BACKGROUND

#### **2.1 Tissue Engineering**

The loss and damage of tissues impairs healthiness of individuals in many different ways. Worldwide, US \$350 Billion are expended for substitute of organs. A typical source for substitution tissue include the patient's own, a donor, or from an animal source. However, there is a scarcity of matched donors and also the risk of infections by viruses (such as HIV, hepatitis C) or a graft rejection. Artificial implants such as those used in knee or hip or blood vessel replacement, have limitations due to their limited lifespan, insufficient bonding to the surrounding tissue, and allergic reactions caused by material abrasion. New therapy concepts for practical medical applications are required. To this end, tissue engineered substitutes generated outside the body could open new strategies for the restoration of damaged tissues.

The goal of tissue engineering is the development of cell-based substitutes to restore, maintain or improve tissue function. These substitutes should have organ-specific properties with respect to biochemical activity, microstructure, mechanical integrity and bio stability. Cell based concepts include the (i) direct transplantation of isolated cells, (ii) implantation of a bioactive scaffold for the stimulation of cell growth within the

original tissue and (iii) implantation of a three dimensional bio hybrid structure of a scaffold and cultured cells or tissue (Portner, Nagel-Heyer et al. 2005). The basic principle of tissue engineering is illustrated in **Figure 2.1**.

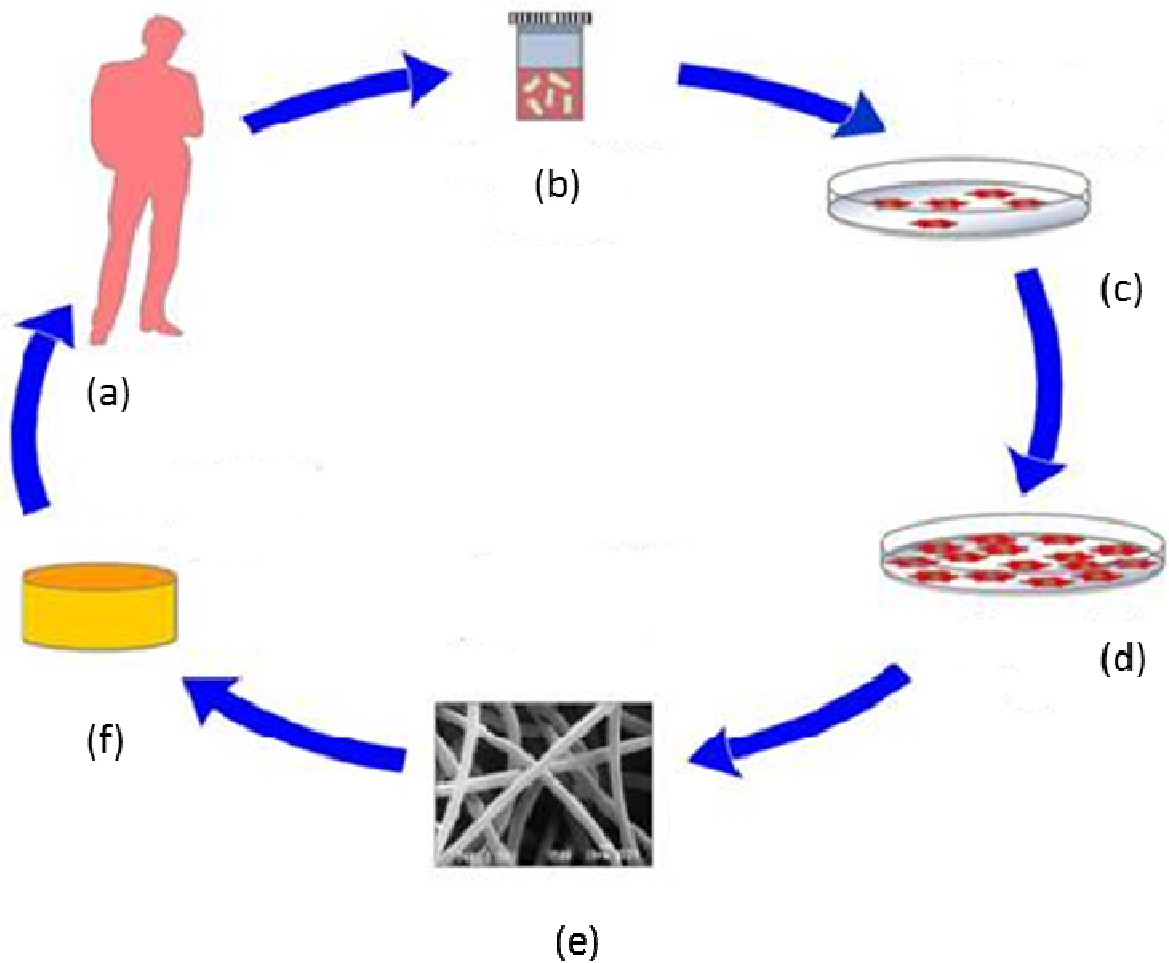


**Figure 2.1 Basic principle of Tissue engineering. (a) Patient, (b) Cells from a biopsy, (c) Monolayer cell culture, (d) Expanded cells, (e) Culture on a 3D polymeric scaffold, (f) Generation of a graft (2008).**

Stem cells or mature cells from the tissue to be regenerated are populated in a petri-dish using the growth media until sufficient number of cells is formed. The medium used

typically contains electrolytes, glucose, hormones, growth factors, and essential amino acids, similar to that in the body. Oxygen from the environment is allowed to dissolve and diffuse in the medium constantly. Once there is enough number of cells, they can be seeded on a polymeric scaffold to provide cell attachment, differentiation or growth in a bioreactor. In the bioreactor, growth medium is constantly mixed either by fluid flow or agitator. When the construct is mature enough, then it is implanted in the area of defect in patient's body.

## **2.2. Porous scaffolds**

Scaffolds are the temporary porous structures necessary to support the maturation of cells into tissues in the desired shape and thickness. The primary constituent of scaffold is a biodegradable material that can either be obtained from natural sources such as exoskeletons of shrimps and crab shells (Devarapalli 2008) or synthesized artificially. Material used to build scaffold should be bio-compatible, bio-degradable, allow cell attachment and tissue formation without any inflammatory or toxic response (Freed LE 1994a; Sawtell RM 1995; Chapekar 2000; Agarwal CM and Ray 2001). With respect to the mechanical properties, it should be strong enough to withstand the process of implantation and the loads it will experience in vivo (Chapekar 2000; Agarwal CM and Ray 2001; Freyman T M, IV et al. 2001; Kuo CK and PX. 2001). The scaffold microenvironment should mimic to that of native tissue condition. One important attribute of the scaffold is permeability and it facilitates in diffusion of nutrients into the matrix and removal of metabolic and degradation by-products from it (LeBaron RG and KA 2000). Permeability depends on the porosity, the type and size of pores. Large

number of interconnected pores are necessary for the cells to be able to infiltrate the structure uniformly (Freed LE 1994a; Chapekar 2000; Kuo CK and PX. 2001). Also the size of pores within the scaffold is important for the attachment and growth of cells. It is intended to build open pores as it has nutrient –access on both sides and also for better cell infiltration.

Material used for this study is a polymeric blend of chitosan and gelatin. Chitosan-based scaffolds has been explored in various tissue engineering applications due to a number of advantages they offer, including cost, large-scale, anti-microbial activity, availability, superior mechanical properties and biocompatibility (Khor and Lim 2003; Kim, Seo et al. 2008). Chitosan is a bioactive, biocompatible, and biodegradable polysaccharide (Khor and Lim 2003). Chitosan is similar in structure to that of glycosaminoglycan present in the extracellular matrix (ECM) and is readily available from various sources (D.L. Nettles, S.H. Elder et al. 2002). Chitosan can be processed into different forms such as porous scaffolds, injectable gels, nanofibers, or films (Ratakonda, Sridhar et al. 2012). The required porous microstructure, biological activity and mechanical strength of chitosan can be achieved by varying the concentration of chitosan, degree of deacetylation, and blending with other materials(D.L. Nettles, S.H. Elder et al. 2002). For instance, chitosan–gelatin scaffolds have also been used (L.J. Dortmans, A.A. Sauren et al. 1984; J.S. Mao, L. Zhao et al. 2003) to incorporate cell adhesion and migration properties of gelatin (Shigemasa, Saito et al. 1994; Chung, Yang et al. 2002; J. Li, J. Pan et al. 2003), since gelatin contains Arg-Gly-Asp (RGD) like sequence that improves the biological activity (Huang, Onyeri et al. 2005). Also addition of gelatin to chitosan can make the scaffolds withstand higher stresses (Ratakonda, Sridhar et al. 2012). Chitosan-

gelatin solution can be prepared by dissolving in dilute acids since for  $\text{pH} < 6$ , the compound becomes protonated and hence soluble (Madihally and Matthew 1999).

There are several techniques available to manufacture porous templates such as solvent casting and particulate leaching, emulsification/freeze-drying, computer aided design, phase separation, nanofibers self-assembly and textile technology (Hong and Madihally 2011). The technique used to prepare chitosan-gelatin scaffold is controlled rate freezing and lyophilization technique (CRFLT) as it has been extensively studied in the laboratory (Madihally and Matthew 1999; Huang, Onyeri et al. 2005; Tillman, Ullm et al. 2006). This technique is also useful, because both the pore alignment and the pore size can be controlled (Madihally and Matthew 1999). In CRFLT, the polymer solution is cooled below its melting point and then lyophilized to sublimate the solvent and thereby forming a porous structure. The pore diameter can be controlled by varying the freezing temperature (Madihally and Matthew 1999) and alignment of the pores depends on the direction of cooling, since the crystal growth will be in the direction of heat transfer. Different concentrations of chitosan-gelatin scaffolds ranging from 0.5% to 2 % had been tested (Ratakonda, Sridhar et al. 2012) and 2%-2% chitosan-gelatin scaffold is used in this study since it is shown to have conducive properties for cell colonization. Characteristics such as the porosity, size of the pores and permeability of the 2%-2% chitosan-gelatin scaffold is also well-established in the laboratory (Dhane 2010).

### **2.3. Bioreactors in Tissue engineering**

Bioreactors are generally defined as devices in which biological and/or biochemical processes develop under closely monitored and tightly controlled environmental and

operating conditions (e.g. pH, temperature, pressure, nutrient supply and waste removal). The requirements of the bioreactors for tissue regeneration include meeting the specific criteria for 3D tissue constructs based on cells and scaffolds, including the proliferation of cells, seeding of cells on macro-porous scaffolds, nutrient (particularly oxygen) supply within the resulting tissue, and mechanical stimulation of the developing tissues (Martin, Wendt et al. 2004). Mechanical stress plays an important modulatory role in certain cells, primarily those exposed to different types of stresses in the body. For example, bones in the lower legs are under constant compressive stress while the blood vessels are under constant hydrodynamic stress. The application of hydrodynamic stress is shown to improve ECM secretion in chondrocytes (Cioffi, Boschetti et al. 2006). Thus bioreactors are also utilized to apply stresses of required level in different configurations.

There are several types of bioreactors in use such as static culture techniques, rotary vessels and perfusion flow systems. Static culture techniques using petri-dishes have limitations of tissue growth localized to the construct periphery (Ishaug SL 1997) mainly due to the inadequate distribution of nutrients (Freed, Marquis et al. 1993; Pazzano, Mercier et al. 2000). Rotary vessels such as slow turning lateral vessels and high aspect ratio vessels have problems such as inhomogeneous tissue growth and improper nutrient distribution (Devarapalli 2008). Perfusion flow systems such as parallel flow, flow through and axial flow has several advantages such as

- i) enhancing nutrient transport as they allow medium to be transported through the interconnected pores of the scaffolds (Bancroft GN 2003),
- ii) providing mechanical stimulation to the cells by applying fluid shear stresses that depend upon flow rate of the perfusing medium [30] and



iii) support culturing high-aspect ratio tissues (which are the case in most tissue types) with high cell density and large cell-numbers as they are required to achieve physiologically meaningful functions in tissue engineering (Griffith and Naughton 2002; Strain and Neuberger 2002).

These bioreactors utilize a pump to perfuse medium continuously through the interconnected porous network of the seeded scaffold. The fluid path must be confined so as to ensure the flow path is through the scaffold, rather than around the edges. A circular cross-section of the bioreactor is preferred as it does not have edges and this minimizes dead zones. The dead zones in the bioreactor lead to cell death or necrosis.

Flow-through and parallel-flow bioreactors (**Figure 2.2**) have been previously studied (Devarapalli 2008; Podichetty 2009). These two types of bioreactors possess the capability to grow complex tissues (tissue that contain more than one cell type). In parallel-flow bioreactors, fluid flows on top of the porous scaffold, applying wall shear stress at the top surface (Dhane 2010). These bioreactors are adapted from flow-chambers used in vascular studies where the cells were attached to the surface. Many modifications have been attempted while introducing porous scaffolds such as adding a medium reservoir below the scaffold, circulating fluid both sides of the scaffold either in steady state, or in oscillation. Some applications include cartilage, bladder and skin (Devarapalli 2008), since there is possibility of controlling the wall shear stresses. The high degree of structure heterogeneity usually noticed in 3D-engineered constructs cultured in static conditions (i.e., presence of a necrotic central region, surrounded by a dense layer of viable cells) suggests that diffusional transport does not properly ensure uniform mass transfer within the constructs (Wendt, Riboldi et al. 2011). Since the

nutrient distribution to the interior of the scaffold is dictated by diffusion, parallel-flow bioreactors are restricted by the porosity of scaffold, which significantly influences effective diffusivity. Some studies have shown reduced oxygen availability for lower values of pore size and porosity. The split channel designs (parallel-flow on both sides of the scaffold) allow better nutrient distribution with lower pressure drop. Increase in scaffold thickness has a negative effect on nutrient distribution in parallel-flow reactors. In flow-through bioreactors, fluid flows through the pores of the scaffold along the diameter. The flow-through bioreactor is better suited for regenerating high aspect ratio tissues due to (Lawrence, Devarapalli et al. 2009): (i) providing uniform support to the scaffold, and (ii) continuously replenishing the nutrients while providing better control on hydrodynamic shear stress induced by the fluid flow. Hence, flow-through bioreactors have generated significant interest in bone regeneration applications, where scaffolds could withstand high fluid flow rate. Use of flow-through bioreactors is essentially dependent on the mechanical strength of the scaffold. Since the fluid has to pass through a porous medium of narrow channel for a longer distance, very high flow rates are necessary to overcome the pressure drop across the scaffold. Although flow-through bioreactor has convective flow, at higher flow rates it has high pressure drop and shear stress that might wash away the newly secreted matrix elements prior to their assembly (Devarapalli 2008). Some modifications in the shape, size, and the number of scaffolds have been tested; however, using these bioreactor configurations is restricted by the scaffold mechanical properties.

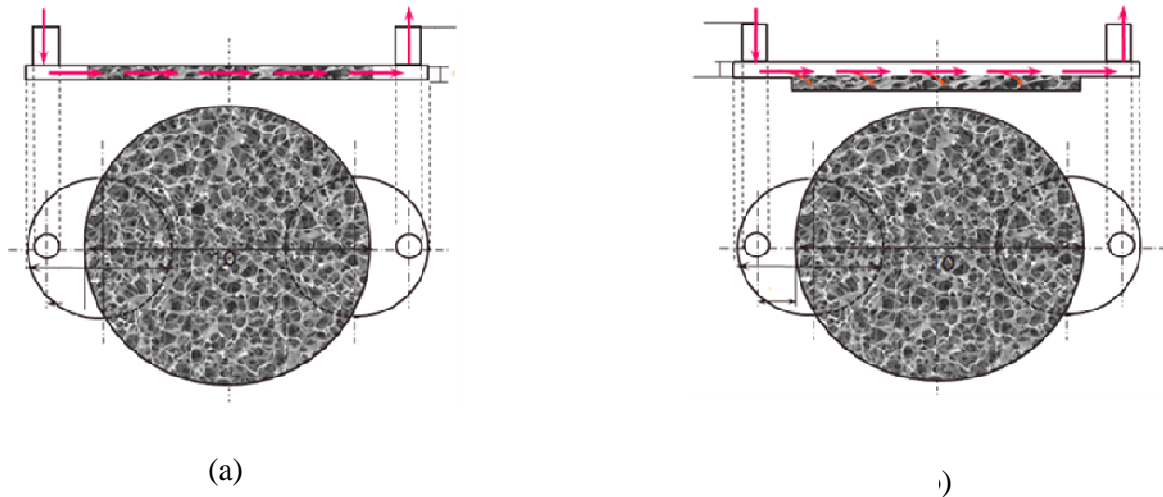
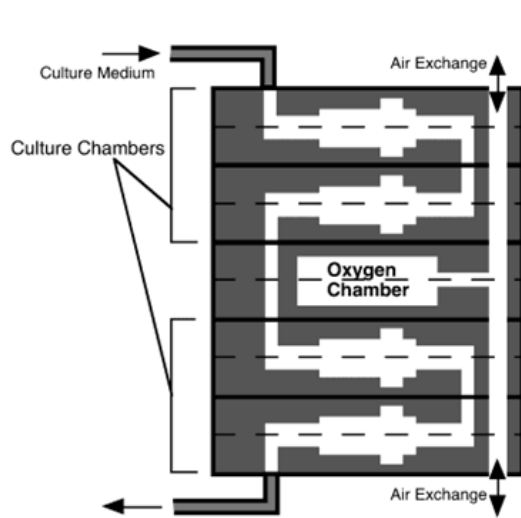
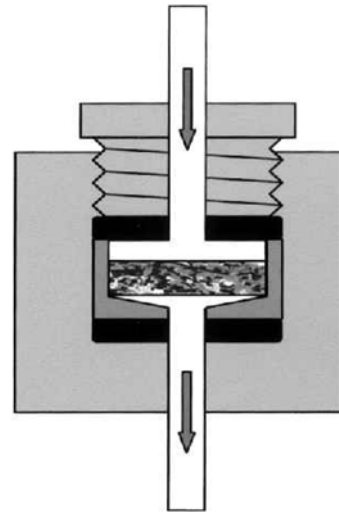


**Figure 2.2. (a) Flow Through Bioreactor, (b) Parallel Flow Bioreactor**

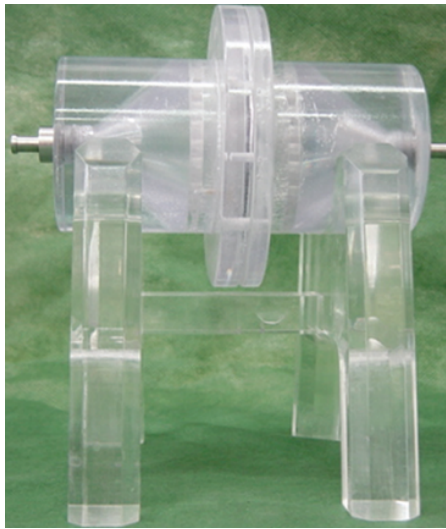
Alternatively, changing the flow configuration to axial direction is advantageous as fluid has to pass only through the thickness of the scaffold. Hence the pressure drop would be significantly reduced. These bioreactors will be referred as the axial-flow bioreactors. Axial-flow bioreactors can be operated at high flow rates as there will be less pressure drop and shear stress. Axial flow type can be useful to culture highly metabolic active cells which require a high replenishment of nutrients. Some configurations of axial bioreactors have been explored to regenerate various tissues (**Figure 2.3**). These bioreactors have different inlet and outlet diameters, different scaffold diameters and different entry semi-angles. Systematic analysis of the influence of various geometric ratios, however, has not been explored in these bioreactors. Even when modeling was performed to explain the hydrodynamic characteristics, porous region was not considered for in the governing equation. Also, nutrient distribution patterns in these bioreactors have not been modeled. The challenge in axial flow bioreactors is obtaining the uniform distribution of nutrients throughout the region of the scaffold. In addition these bioreactors are less than 50 mm in diameter and effect of scaling up the reactor has not been investigated.



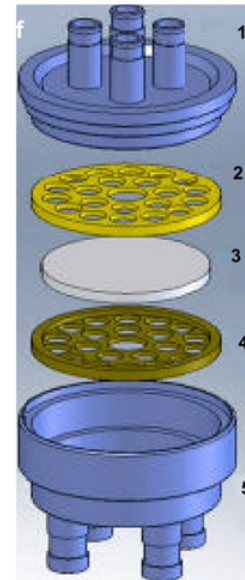
(a)



(b)



(c)



(d)

**Figure 2.3 Axial flow bioreactors in use. (a) Microfluidic bioreactor for large scale culture of hepatocytes (Leclerc, Sakai et al. 2004), (b) bioreactor for bone tissue-engineering applications,(Bancroft GN 2003) (c) perfusion bioreactor for cardiac cell (Dvir T 2006), and (d) perfusion bioreactor for abdominal wall cells (Pu, Rhodes et al. 2010).**

The current requirements in the design of axial-flow bioreactor are as follows:

- i) modeling the bioreactor to study the fluid flow characteristics separately in the porous and non-porous domain
- ii) scaling up of the bioreactor to accommodate various sizes of scaffolds (both thickness and diameter) necessary for regenerating various tissues
- iii) minimizing the bioreactor hold-up volume
- iv) studying the influence of geometry of the bioreactor on fluid flow characteristics and nutrient distribution
- v) evaluating the effect of changing porous characteristics of the scaffold during the regenerative process
- vi) understanding the influence of medium flow rates and
- vii) ensuring the uniform shear stress and nutrient distribution throughout the region of the scaffold for different types of cells

The objective of this study was to perform detailed analyses on various factors in modeling the axial-flow bioreactor.

## **2.4 Computational Fluid Dynamics Simulation**

Evaluating the hydrodynamic characteristics and the distribution of nutrients is essential to predict the efficacy of the bioreactor in regenerating a desirable tissue. Although experimental methods are reliable, it is time consuming in terms of characterizing the complete 3D fluid flow within a bioreactor. The computational methods such as simulation are powerful and cost-effective method used for modeling and optimizing the design of the bioreactor. The use of computational methods to predict and understand the

flow-dependent processes in the bioreactor can improve the overall performance of the system, and reduce both the time and cost of development (Martin and Vermette 2005). In addition they allow a faster design approach by modeling different configurations and generating visual results for a better understanding (Hidalgo-Bastida, Thirunavukkarasu et al. 2012). However, the influence of various parameters on fluid distribution and nutrient sufficiency in the bioreactor are not explored while designing axial-flow bioreactors.

A more detailed description of fluid mechanics and nutrient transport can be achieved using Computational Fluid Dynamics (CFD) technology (Hutmacher and Singh 2008). The method used in this technique is to discretize the fluid domain into smaller finite elements like mesh and use iterative method to solve the equations governing fluid flow. Several bioreactor designs can be evaluated and characterized using CFD prior to fabrication and experimentation. CFD modeling involves choosing i) the dimensions of the reactor, ii) appropriate governing equations with boundary conditions, iii) the values for the constants involved in the governing equation, and iv) necessary tool to solve these equations for different dependent variables. In addition, specific parameters such as inlet medium flow rates and shear stresses can be varied to better predict their influence and thereby optimizing tissue growth (Hutmacher and Singh 2008). CFD technique can also be useful in evaluation of parameters in some locations inside the bioreactor where it is impossible to position probes for experimental measurement. Since cell growth is a dynamic process, the effect of certain parameters such as pressure drop on permeability can also be evaluated using CFD technique.

## 2.5 Fluid Flow Characteristics

The bioreactor uses mechanical stimulation to obtain de novo tissue with biomechanical properties comparable to the damaged or desired tissue. Mechanical stimulation techniques involve subjecting a scaffold to mechanical stresses resembling the in vivo environment. It is shown that applying mechanical stimulation by subjecting a scaffold to dynamic flow provides a uniform cell distribution throughout the three dimensional seeded construct resulting in a homogenous matrix deposition (Martin, Wendt et al. 2004). It is necessary to study the hydrodynamic characteristics to evaluate parameters such as shear stress which can influence the growth of cells.

Navier-Stokes equation explains the fluid behavior in non-porous regions.

$$-\nabla P + \eta \nabla^2 v + F = 0 \quad (2.1)$$

where  $P$  is the pressure,  $F$  is any external forces acting on the fluid,  $v$  is the velocity and  $\eta$  is the viscosity. They are useful to calculate the pressure drop profiles, the shear stress at various points in the bioreactor and also the velocity profiles. The walls of the bioreactor are assumed to be rigid and hence the condition ‘no slip at the walls’ holds true.

Darcy’s law describes the flow of a fluid in a porous medium (Equation 2.2)

$$v = \frac{-k(\nabla P)}{\eta} \quad (2.2)$$

where  $k$  is the permeability of the porous medium. There is a problem in using Navier-Stokes and Darcy’s law equations together, since the order of these equations are not equal and hence will not be able to maintain continuity at the free/porous interface. This can be eliminated by using Brinkman equation which has the same order as the Navier-Stokes equation and hence the continuity in the mass flux and stress can be applied at the

free/porous interface (Hidalgo-Bastida, Thirunavukkarasu et al. 2012). Also Brinkman equation makes sure that the viscous stress experienced within the fluid is included when permeability is large.

Brinkman equation 2.3 is formed when the pressure drop term from the Darcy's law is replaced in the external force term of Navier-Stokes Equation (Capuani, Frenkel et al. 2003).

$$-\nabla P + \eta \nabla^2 v - \frac{\eta v}{\kappa} = 0 \quad (2.3)$$

When the permeability is infinite the last term in the above equation is zero and the equation 2.3 reduces to Navier-Stokes Equation and when the viscous forces or the second term in the above equation is negligible, equation 2.3 reduces to Darcy's law. The permeability values depend upon the type of pores and it can be calculated from Poiseuille's and Darcy's law for cylindrical pores and Kozeny-Carman equation for non-cylindrical pores (Truskey GA 2004).

It is also known that fluids diffuse through the porous medium. Hence, prediction of diffusion coefficients in the porous medium is essential. This can be found out using the diffusion models based on electric conductivity by Maxwell (Maxwell and Garnett 2011) and Fricke (Fricke 1924) or models based on tortuosity in a simple cubic lattice model by Mackie and Meares (Mackie and Meares 1955; Mackie and Meares 1955), because these two models give a simple dependence of the reduced diffusion coefficient on the polymer volume fraction (Waggoner, Blum et al. 1993). Since Mackie-Meares relationship has a simpler expression, this model is used. Before using this equation, it is necessary to know the infinite diffusivities which can be calculated from Stokes-Einstein equation.



## 2.6 Nutrient Distribution with Consumption

Nutrient media is critical for the survival of cells. The bioreactor design has to ensure that nutrients are uniformly distributed throughout the region of the scaffold. The consumption of nutrients depends upon the type of cells cultured. To understand the consumption patterns, studying of reaction kinetics is essential. Studying consumption of oxygen and glucose are critical since oxygen is required for cellular respiration and glucose is the major energy source for the cells. Since, perfusion systems ensure a continuous supply of nutrients, the concentration of nutrients is determined by their flow rate. It has to be understood that the nutrients in the flow media, are both being convected and diffused. So the concentration of nutrients at any position in the bioreactor can be predicted using the convection-diffusion equation.

Consumption rate for both oxygen and glucose is predicted by the Michaelis-Menten kinetics. Since this study aims at building a more efficient perfusion bioreactor by comparing it with the previous studies, the reaction rate constants based on smooth muscle cells were used similar to parallel and flow through bioreactors (Devarapalli 2008; Podichetty 2009).

The inlet concentration for oxygen for smooth muscle cell was found to be  $0.22 \text{ mol/m}^3$  by using Henry's law to find the solubility of oxygen in water at  $37^\circ\text{C}$  and 1 atm and the inlet concentration of glucose was found out as  $5.5 \text{ mol/m}^3$  based on the growth media formulations (Devarapalli, Lawrence et al. 2009). The inlet flow rates of the nutrient medium are calculated using equation 2.4 which is based on the desired concentration of oxygen in the outlet and this depends on the type of cell cultured.

$$-r_{O_2, Inlet} = \frac{v\Delta C_{O_2}}{V_R} \quad (2.4)$$

where,  $v$  is the volumetric flow rate,  $V_R$  is the volume of the bioreactor and  $\Delta C_{O_2}$  is the desired change in concentration of Oxygen at the bioreactor outlet. The left hand side of the equation is the Michaelis-Menten rate law at the inlet concentration. For smooth muscle cells with desired outlet concentration of  $0.07 \times 10^{-6}$  mol/mL (Devarapalli, Lawrence et al. 2009), the inlet volumetric flow rate was found out to be 0.1 mL/min.

## **2.7 Importance of Residence Time Distribution**

Perfusion bioreactors dealt in this study have a high-aspect ratio with large scaffold diameter relative to the thickness. As the scaffold size increases, the fluid distribution can become non-uniform caused mainly due to two factors: i) channeling and ii) dead zones (Lawrence, Devarapalli et al. 2009). These types of non-uniform flow results in improper distribution of nutrients and non-uniform shear stress distribution which must be avoided as it always lowers the performance of the unit (Levenspiel). Channeling occurs when some of the fluid molecules bypass the bioreactor without dispersing in the entire volume of the reactor. Dead zones are created when the fluid does not reach certain regions of the bioreactor and thereby reducing the effective volume of the bioreactor. If dead zones occur in regions where cells are present, decreased nutrient transport leads to the cell death or necrosis and it will affect the quality of the surrounding cells as well.

To understand the fluid distribution in a reactor, residence time distribution (RTD) analysis is performed. Residence time of the reactor is the time the molecules have resided in the reactor. Since different molecules reside for different times based on their distribution, a distribution in time is obtained. RTD does not depend on the type of cells,

but only depends on the fluid distribution characteristics of the bioreactor. RTD signifies the amount of time the cells and the nutrients are in contact (Devarapalli, Lawrence et al. 2009).

Mean residence time,  $t_m$  can be calculated from RTD, which explains the mean time the molecules spend in the bioreactor. If the molecules are distributed in the entire volume of the bioreactor, ideal residence time (also called space time),  $\tau$ , can be calculated using the ratio of the volume of the reactor to the flow rate of the growth medium. Ideally, the mean residence time  $t_m$  should be equal to the space time of the reactor,  $\tau$ . Comparing the mean residence time to the ideal space time provides information on the nutrient distribution characteristics. Decreased  $t_m$  can be attributed to different phenomena such as dead zones and channeling which results in less consumption of nutrients. So an ideal design of the bioreactor is a one, which has space time nearly equal to the mean residence time. Distribution of nutrients in the reactor has to be uniform throughout the region of the scaffold in the bioreactor to ensure homogeneity of the cells.

## CHAPTER III

### OPTIMIZATION OF BIOREACTOR VIA CFD SIMULATION

#### 3.1 Introduction

The objective of this study was to simulate an axial-flow bioreactor that could support high aspect ratio scaffold for tissue regeneration. Since nutrients are vital for the survival of cells, the bioreactor design must have uniform nutrient distribution throughout the scaffold. In addition, it is necessary to minimize the volume of the bioreactor to decrease the holdup volume of the expensive media.

To fulfill these objectives, several parameters such as diameter of the bioreactor and semi-angle of the cone were varied. In each analysis, the volume of the bioreactor ( $V_R$  in mL), outlet oxygen concentration ( $C_{O_2, Out}$  in  $\text{mol/m}^3$ ), maximum shear stress in the scaffold ( $\tau$  in  $\text{dyne/cm}^2$ ) and pressure drop ( $\Delta P$  in Pa) across the bioreactor were evaluated from the simulation results. Based on these evaluations, a configuration suitable for housing high aspect ratio scaffolds was selected for further analyses. The effect of inlet diameter, outlet diameter, thickness of the scaffold, flow rate of the nutrient medium, and permeability of the scaffold were evaluated. Based on these analyses, changes were incorporated into the bioreactor design

## 3.2 Setting the Simulation

Simulation was set up using the following steps (Figure 3.1)

1. Drawing the bioreactor shape
2. Governing Equations and the Boundary Conditions
3. Meshing the system
4. Post-processing the Results

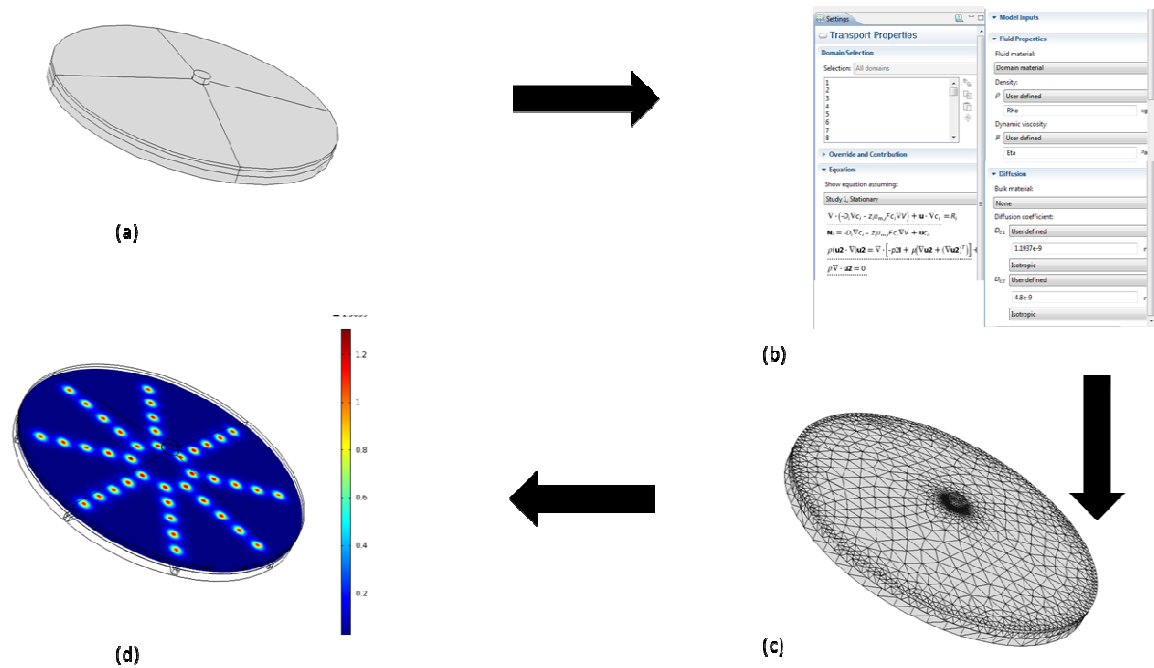


**Figure 3.1 Steps involved in CFD Simulation. (a) Drawing the system in the model view, (b) Governing Equations and the Boundary Conditions, (c) Meshing the system, (d) Post-processing the results**

### 3.2.1 Creating the Bioreactor Design

COMSOL Multiphysics v 4.2 was used to create the axial flow bioreactor design. Step by step procedure for drawing the bioreactor is described in **Appendix A**. In brief, *Reacting*

*Flow, Diluted Species* the module was selected, which integrated free and porous media flow (Fluid dynamics) and transport of diluted species (Reaction Engineering) physics.

Bioreactor geometry had 6 regions: the inlet, the bottom cone, the porous scaffold, hold up region, top cone and the outlet.

### 3.2.2 Selection of Governing Equations and the Boundary Conditions

The governing equations and constants used in this study were similar to the previously described conditions (Devarapalli, Lawrence et al. 2009). In brief, nutrient medium was assumed to have the physical properties of water at 37 °C. The *Free and Porous Media Flow* module was used to obtain pressure drop and shear stress profile. The concentration profiles of oxygen and glucose were obtained from *Transport of Diluted Species* module. Since cells are embedded in the scaffold, they were considered to be part of the porous scaffold. The following assumptions were made while applying the equations:

1. Incompressible fluid

Density of the fluid was assumed to be constant which resulted in the special form of continuity as shown by the equation 3.1:

$$(\nabla \cdot v) = 0 \quad (3.1)$$

where  $v$  is the velocity of the fluid.

2. Newtonian fluid

Resistance to flow of fluid was assumed to be given by the Newton's law of viscosity

3. Steady state

It was assumed that the properties of the fluid do not change with time and also there was zero accumulation of any quantity with constant inflow and outflow.

#### 4. Uniform distribution of cells

It was assumed that the seeding of the cells on the porous scaffold was done uniformly so that a constant cell density throughout the region of the scaffold was achieved.

#### 5. Rigid bioreactor walls

It was assumed that the bioreactor walls were rigid so that the no slip boundary condition was valid at the fluid-solid interface.

#### 6. Rigid porous scaffold

It was assumed that the microscopic structure of the porous scaffold did not deform during the process of cell culture.

### 3.2.2.1 Fluid Flow Characteristics

Bioreactor was divided into two domains/regions: porous and non-porous. The fluid flow characteristics in the non-porous region were evaluated by using Navier- Stokes equation:

$$\rho(u \cdot \nabla)u = -\nabla \cdot [-\tau + p\delta_{ij}] \quad (3.2)$$

where  $\rho$  is the fluid density ( $\text{kg/m}^3$ ),  $p$  is the pressure (Pa),  $\delta_{ij}$  is the Kronecker delta function and  $u$  is the velocity in the open channel (m/s). Density of the fluid was taken as  $1000 \text{ Kg/m}^3$  and dynamic viscosity was taken as  $0.0006915 \text{ N s/m}^2$ .

In the porous region, the fluid flow characteristics were governed by Brinkman equation:

$$\nabla p = \mu \nabla^2 u_s - \frac{\mu}{k} u_s \quad (3.3)$$

where  $k$  is the permeability of the porous medium,  $u_s$  denotes the fluid superficial velocity

vector,  $p$  is the fluid pressure and  $\mu$  is the effective viscosity in the porous medium(Truskey GA 2004).

Assuming uniformly distributed cylindrical pores in the scaffold, permeability was calculated using Kozeny equation (Truskey GA 2004),

$$k = \frac{\pi d^4 n_A}{128} \quad (3.4)$$

where  $n_A$  is the number of pores per unit area, and  $d$  is the average diameter. The permeability was calculated for chitosan gelatin scaffold with pore architecture similar to a previous study (Podichetty 2009):

**Table 3.1.Pore Architecture**

No. of pores per mm <sup>2</sup> ( $n_A$ )	318
Diameter( $d$ ) of pores( $\mu$ m)	55
Porosity, $\varepsilon_p$ (%)	77

The initial velocity  $u_0$  was set based on the desired flow rate. The outlet pressure was equivalent to 1atm (or zero gauge pressure) and no slip at the walls was used for the other boundaries.

### 3.2.2.2 Nutrient Consumption Pattern

The concentration of nutrients, oxygen and glucose was evaluated using convective diffusive equation:

$$\nabla \cdot (-D \nabla C_A) + u \cdot \nabla C_A = r_A \quad (3.5)$$

where  $c_A$  is the concentration of species in mol/m<sup>3</sup>,  $D$  is the diffusion coefficient of the



species in water and  $r_A$  is the reaction rate of species A.

From literature (Dhane 2010), the diffusion coefficient for oxygen in water was found to be  $1.1937 \times 10^{-9} \text{ m}^2/\text{s}$  and glucose in water was  $4.8 \times 10^{-9} \text{ m}^2/\text{s}$ . These values were used in the simulation studies. The consumption of these nutrients was assumed to follow Michaelis Menten's equation, and the reaction rate  $r_A$  was given by:

$$r_A = -\frac{V_M C_A}{K_M + C_A} \quad (3.6)$$

where  $V_M$  is the maximum reaction rate ( $\text{mol}/\text{m}^3\text{s}$ ),  $C_A$  is the inlet concentration of oxygen ( $\text{mol}/\text{m}^3$ ) and  $K_M$  is the Michaelis Menten constant ( $\text{mol}/\text{m}^3$ ). From literature, (Motterlini, Kerger et al. 1998; Alpert E 2002a; Devarapalli, Lawrence et al. 2009) rate constants  $K_M$  and  $V_M$  for oxygen and glucose for smooth muscle cells were obtained for cell density of  $1.2 \times 10^{12} \text{ cells}/\text{m}^3$ . These kinetic parameters are listed in **Table 3.2**.

**Table 3.2. Rate Constants for Smooth Muscle Cells**

	Glucose	Oxygen
$V_M(\text{mol}/\text{m}^3.\text{s})$	$4.862 \times 10^{-5}$	$3.164 \times 10^{-5}$
$K_m(\text{mol}/\text{m}^3)$	0.93	0.205

An inlet oxygen concentration of  $0.22 \text{ mol}/\text{m}^3$  was used based on calculations using Henry's law at  $37^\circ \text{C}$  and an inlet glucose concentration of  $5.5 \text{ mol}/\text{m}^3$  was used based on the growth media formulations utilized in culturing smooth muscle cells. These values were used as the boundary conditions for solving this system. To account for the constant cell density in the scaffold with various diameters and sizes,  $V_M$  was calculated using appropriate number of cells as described in Section 3.3.1.

### **3.2.3 Meshing the System**

Finite element method (FEM) in COMSOL: Multiphysics v4.2 approximates a partial differential equation problem that has a finite number of unknown parameters, i.e., discretization of the original problem. The starting point for the finite element method is creating a mesh, partitioning the geometry into small units of a simple shape, such as triangle. These are called (mesh) elements. Since the bioreactor model involved more than one geometric shape, free meshing technique was used. There are three types of free meshing in COMSOL Multiphysics v4.2 namely free triangular, free quadrilateral and free tetrahedral. The free tetrahedral mesh was used for various designs based on the physical settings of the models. Also the simulator selected the size of each mesh element to provide mesh-independent results. The number of nodes for each system changed based on the geometry of each bioreactor model.

### **3.2.4 Generating Results**

After running the simulation, solution for each of the dependent variable involved in the equations were obtained. The desired profiles of the dependent variables namely the pressure drop across the bioreactor, shear stress within the scaffold and concentration of oxygen and glucose were evaluated by creating 3D plot groups. The slice plot option was used to create the 3D- profiles of the dependent variables.

## **3.3 RESULTS**

### **3.3.1 Effect of Increased Scaffold Diameter**

To study the effects of increase in the scaffold diameter, the bioreactor diameter was

scaled up to 2x, 3.5x and 5x mm to accommodate corresponding size scaffolds. For this purpose, the angles and other geometric variations were proportionally increased. However, the inlet and outlet diameters were kept the constant. The total volume of the bioreactor was calculated by adding the volume of each region in the bioreactor as described below. The value of the kinetic parameter  $V_M$  was based on the total number of cells in scaffold of diameter 5x mm and thickness z mm and the cell density of  $1.2 \times 10^{12}$  cells/m<sup>3</sup>. Hence the number of cells and the value of  $V_M$  for 2x and 3.5x mm diameter bioreactor was calculated based on the original cell density.as shown in **Table 3.3**.

**Table 3.3.Values of the Number of Cells and  $V_M$**

Diameter of the scaffold(mm)	Number of cells (Million)	$V_M$ for oxygen ( $\mu\text{mol}/\text{m}^3.\text{s}$ )	$V_M$ for glucose ( $\mu\text{mol}/\text{m}^3.\text{s}$ )
x	0.754	1.26	1.96
2x	3.01	5.06	7.78
3.5x	9.23	15.5	23.8
5x	18.8	31.6	48.6

The effect of scaling up the bioreactor was the increase in bioreactor volume from 4.66 to 319 mL. The **Table 3.4** shows the simulations results performed at a flow rate of 0.1mL/min, and pore size of 55 $\mu\text{m}$  for bioreactors with different diameter of scaffolds. Based on the conservation of mass, velocity would decrease with increased cross sectional area. Since fluid distribution area increased with the scaffold diameter, it resulted in the reduction of hydrodynamic shear stresses in the scaffold. The hydrodynamic shear stress distribution across the scaffold was uniform. Interestingly,

pressure drop across the bioreactor decreased. The uniform distribution of nutrients in the entire scaffold was observed in all the bioreactors. There was a proportional increase in nutrient consumption due to increased cell number. This resulted in decreased outlet oxygen consumption.

Based on the previous work (Devarapalli, Lawrence et al. 2009), minimum volumetric flow ( $v$ ) was calculated using the relation:

$$-r_{O_2}|_{inlet} = v\Delta C_{O_2} / V_R \quad (3.7)$$

where  $V_R$  is the volume of the bioreactor and  $\Delta C_{O_2}$  is the desired change in concentration of Oxygen at the bioreactor outlet. Value of  $(-r_{O_2})_{inlet}$  obtained from the Michaelis-Menten kinetic equation with the constant values from **Table 3.2** was  $16.36 \times 10^{-6}$  mol/m<sup>3</sup>s. The volume of the bioreactor was found using the equation

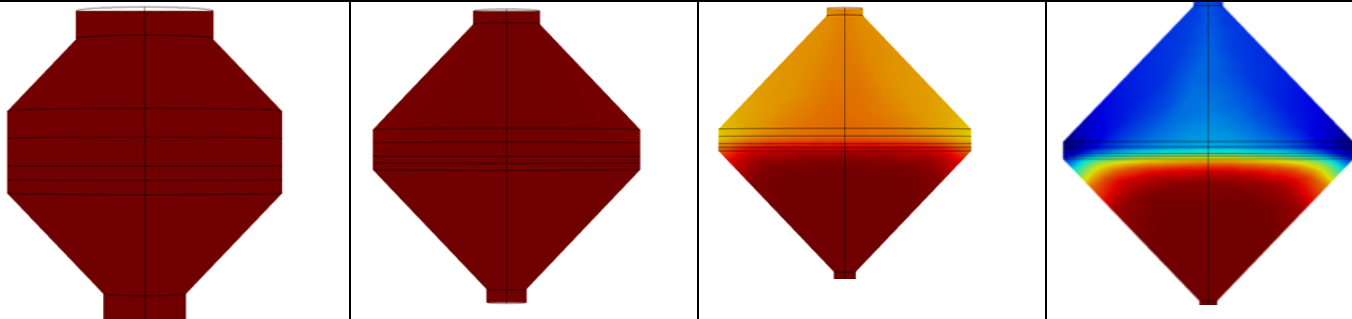
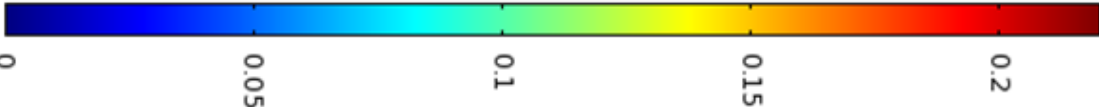
$$V_R = (\pi r_R^2 h \varepsilon_p)_{scaffold} + V_{entry} + V_{exit} \quad (3.8)$$

where,  $r_R$  is the radius of the bioreactor,  $h$  is the thickness of the reactor,  $\varepsilon_p$  is the porosity of the scaffold,  $V_{entry}$  is the volume of the inlet and the entrance cone region which is a frustum whose volume ( $V_{frustum}$ ) is given by the following equation

$$V_{frustum} = \frac{\pi h (Rr + r^2 + R^2)}{3} \quad (3.9)$$

Where  $h$  is the height,  $R$  is the radius of the lower base and  $r$  is the radius of the upper base of a frustum of a cone.  $V_{exit}$  in equation 3.8 is the volume of the outlet and the exit cone region which is again a frustum. Using a desired  $\Delta C_{O_2}$  value of 0.12 mol/m<sup>3</sup>, from equation 3.7, volumetric flow rate was calculated to be 0.1 mL/min.

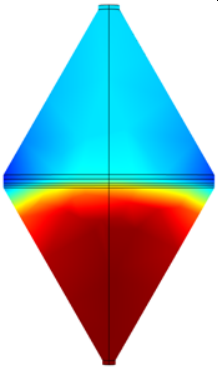
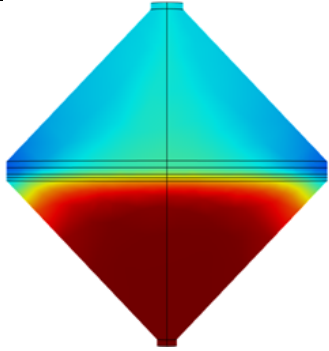
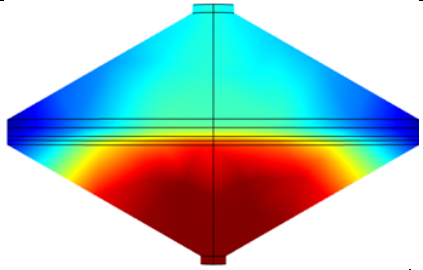
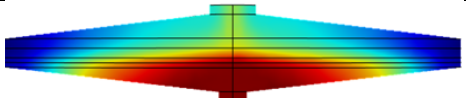
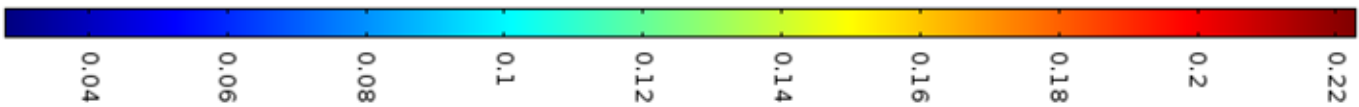
**Table 3.4. Effect of Increased Scaffold Diameter**

<b>D (mm)</b>	<b>x</b>	<b>2x</b>	<b>3.5x</b>	<b>5x</b>
No. of Nodes	92743	127344	144701	154475
$V_R$ (mL)	4.66	14.02	116	319
$\Delta P$ (Pa)	0.09	0.02	0.007	0.004
$\tau$ ( $\mu\text{dyne}/\text{cm}^2$ )	50	11	3	1.4
O <sub>2</sub> Conc. Profile (mol/m <sup>3</sup> )				
				
C <sub>O<sub>2</sub>,Out</sub> (mol/m <sup>3</sup> )	0.219	0.215	0.18	0.099

### 3.3.2. Influence of Semi Angle on Nutrient Distribution

In order to minimize the volume of the bioreactor, semi-angle of the entry and exit cones were varied from  $sa^0$  to  $2.76 sa^0$ , while keeping the inlet and the outlet diameters the same (Table 3.5). As anticipated increasing the semi-angle at the entrance and the exit significantly decreased the volume of the bioreactor. To understand the impact of these changes on fluid flow and nutrient distribution, simulations were performed at a flow rate of 0.1mL/min and a scaffold pore size of 55 $\mu$ m. First, the number of nodes in each bioreactor was increased with semi-angle. However, there was no significant alteration in the pressure drop in any of the bioreactors and the pressure drop ranged in millipascals. On the contrary, a significant increase in the shear stress was observed when the semi-angle was  $2.76 sa^0$ . But this value of shear stress was relatively low to that of flow through configuration (Dhane 2010) which was 1000 $\mu$ dyne/cm<sup>2</sup>. Increasing the semi-angle above  $1.5 sa^0$  showed reduced flow distribution towards the circumference of the scaffold. This resulted in reduced consumption or increase in the outlet oxygen concentration. Hence, a modification in the design was necessary.

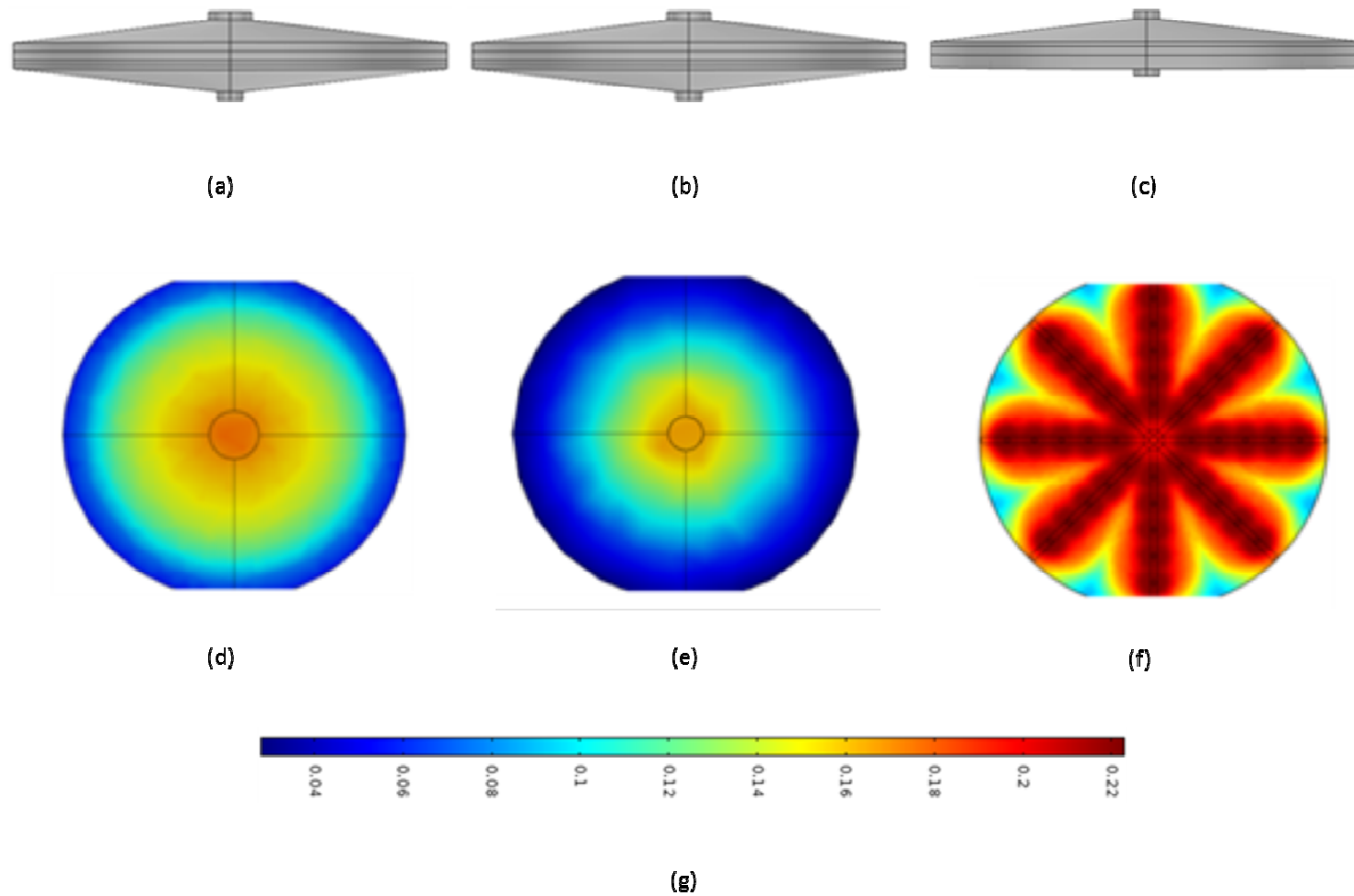
**Table 3.5. Influence of Semi Angle on Nutrient Distribution**

Angle	$sa^0$	$1.5 sa^0$	$2 sa^0$	$2.67 sa^0$
No. of nodes	99174	111068	112892	122488
$V_R(\text{mL})$	496	319	197	77.0
$\Delta P(\text{Pa})$	0.003	0.004	0.004	0.004
$\tau (\mu\text{dyne}/\text{cm}^2)$	1.5	1.6	1.7	30
O <sub>2</sub> Conc. Profile (mol/m <sup>3</sup> )				
				
C <sub>O<sub>2</sub>,Out</sub> (mol/m <sup>3</sup> )	0.097	0.098	0.1	0.12

### 3.3.3. Incorporating a Distribution System

Increase in the semi-angle of the entry and exit shapes reduced the volume of the bioreactor while not providing uniform nutrient distribution (**Figure 3.2 (a)**). To improve the nutrient distribution in these bioreactors, modifications were considered in the section immediately below the scaffold. Initially, this cross-section did not have any distributor systems. Hence, concentric baffles were inserted at regular intervals to regulate the flow. Yet, the distribution was not satisfactory as seen from **Figure 3.2(e)**. Hence, a bioreactor with distributor system (**Figure 3.2(c)**) was designed. To make the construction simpler, conical structure beneath the scaffold was eliminated and was replaced with a cylindrical structure having a thickness of  $z$  mm. On this cylindrical structure, eight distributors in the form of a cuboid were inserted with equally spacing. Each distributor had  $z$  mm width,  $z$  mm depth and  $z$  mm long. Upon, this, were the outlets for the nutrient medium which were in the form of cylinders having  $0.5z$  mm height and a base diameter of  $0.75z$  mm. The nutrient distribution for this design (**Figure 3.2(f)**) was satisfactory as it had uniform distribution throughout the region of the scaffold which can be seen from the scale in **Figure 3.2(g)** showing the concentration of oxygen in  $\text{mol/m}^3$ .



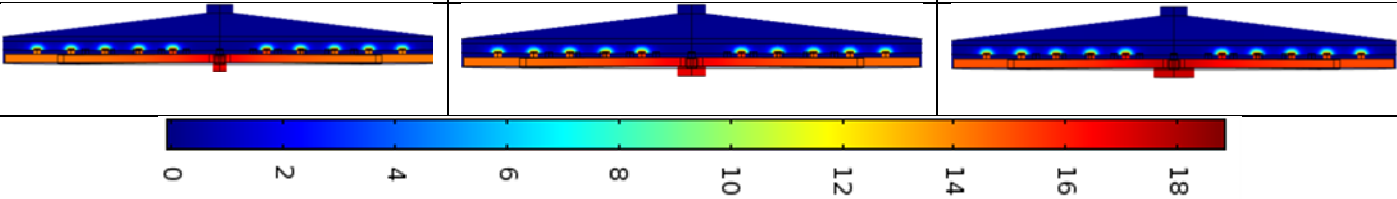


**Figure 3.2 Effect of bioreactor design on nutrient distribution.(a) to (c) Side view of the bioreactor, (d) to (f) Oxygen Concentration. Profile across the scaffold in the region immediately beneath the scaffold , (g)  $\text{CO}_2$  in  $\text{mol/m}^3$**

### **3.3.4 Effect of Changes in Inlet and Outlet Diameters**



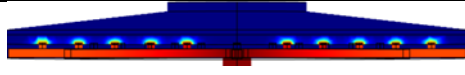

In the new design of the axial-flow bioreactor, the effects of changing the inlet diameter (id, 2id and 3id mm) and the outlet diameter (od, 2od and 3od mm) were studied independently. The semi-angle of the cone was proportionally changed keeping the height constant. Observed simulation results are shown in **Table 3.6** and **Table 3.7**. Overall, no effects with change in inlet diameter or the outlet diameter were observed in the pressure drop, maximum shear stress and the nutrient distribution pattern. Hence, the initial design was used in subsequent studies.

**Table 3.6. Effect of Inlet Diameter on Pressure Drop and Nutrient Concentration**

Diameter(mm)	id	2id	3id
No. of nodes	382484	400781	421787
$\Delta P$ (Pa) Profile			
$\Delta P$ (Pa)	18.8	17.0	17.5
$\tau$ ( $\mu\text{dyne}/\text{cm}^2$ )	$3 \times 10^5$	$3 \times 10^5$	$3 \times 10^5$
$C_{\text{O}_2, \text{Out}}$ ( $\text{mol}/\text{m}^3$ )	0.219	0.219	0.219

Each of the above bioreactors had a hold-up volume of 61.5mL and the simulations were performed for a flow rate of 25 mL/min and pore size of 55  $\mu\text{m}$ .

**TABLE 3.7. Effect of Outlet Diameter on Pressure Drop and Nutrient Concentration**

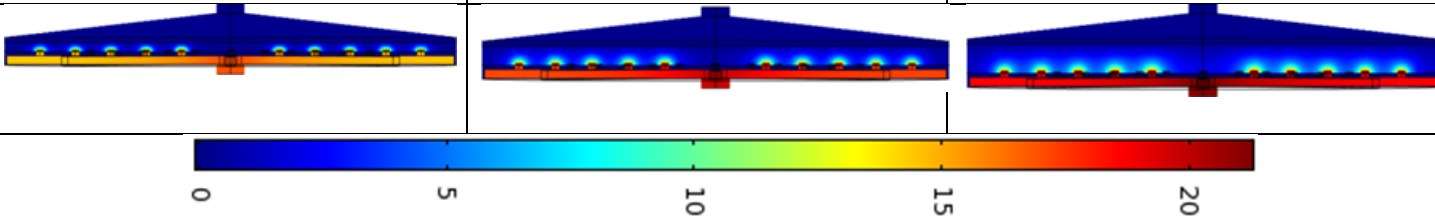
Diameter(mm)	od	2od	3od
No. of nodes	117516	585617	75730
$\Delta P$ (Pa) Profile			
			
$\Delta P$ (Pa)	14.2	14.2	14.2
$\tau$ ( $\mu\text{dyne}/\text{cm}^2$ )	$3 \cdot 10^5$	$3 \cdot 10^5$	$3 \cdot 10^5$
$C_{\text{O}_2, \text{Out}}$ ( $\text{mol}/\text{m}^3$ )	0.217	0.217	0.218

Each bioreactor had a hold-up volume of 61.5mL and the simulations were performed for a flow rate of 25 mL/min and pore size of 55  $\mu\text{m}$ .

### 3.3.5 Influence of Scaffold Thickness

Tissues come in different thickness. To understand the possibility of growing different thickness of tissues, scaffold thickness was increased from  $z$  to  $3z$  mm and simulations were repeated. All other dimensions were kept constant including inlet and outlet diameter and semi-angle. Further, the cell density was kept constant i.e., number of cells in the reactor was proportionally increased with thickness. These results (**Table 3.8**) showed that increase in thickness marginally increases pressure drop across the reactor. However, shear stress did not change as the same volumetric flow rate was used. Despite increase in number of cells to maintain constant cell density, there was no significant decrease in the outlet concentration of oxygen. This suggested that the flow rate is sufficient to grow tissues up to  $3z$  mm thickness and no additional changes are required.

**Table 3.8. Effect of Scaffold Thickness on Pressure Drop and Nutrient Concentration**

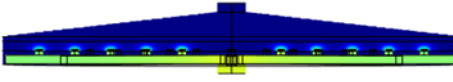
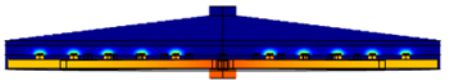
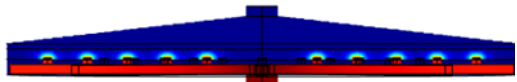

Scaffold Thickness (mm)	$z$	$2z$	$3z$
No of nodes	400781	436670	385673
$V_R$ (mL)	61.59	77.09	92.67
$\Delta P$ (Pa) Profile			
$\Delta P$ (Pa)	17	19.9	21.4
$\tau$ ( $\mu$ dyne/cm <sup>2</sup> )	$3 \cdot 10^5$	$3 \cdot 10^5$	$3 \cdot 10^5$
$C_{O_2, Out}$ (mol/m <sup>3</sup> )	0.219	0.215	0.210

All the simulations were performed at a flow rate of 25mL/min and a pore size of 55  $\mu$ m.

### 3.3.6 Effect of Flow Rate

The flow rate of the nutrient medium was increased from 5mL/min to 25 mL/min. As increase in flow rate exposes the cells to higher shear stress and pressure drop, these two become important parameters for this particular study. From the results, it was observed that as the flow rate increases, the pressure drop across the bioreactor also increases, which is explained by the Hagen-Poiseuille equation. The **Table 3.9** shows the effect of flow rate on pressure drop and nutrient concentration. Dimensionless numbers such as Reynolds and Peclet numbers were calculated at 25 mL/min. Maximum Reynolds number measured was 10.2 which shows that the flow was laminar. Peclet number measured at the middle of the scaffold for oxygen was 45.83 and for glucose was 11.46 which imply that the nutrient flow through the porous scaffold was convection dominant.

**Table 3.9.Effect of Flow Rate on Pressure Drop and Nutrient Concentration**

FlowRate (mL/min)	15	20	25
No. of nodes	400781	400781	400781
$\Delta P$ (Pa)  Profile			
			
$\Delta P$ (Pa)	10.0	13.5	17.0
$\tau$ ( $\mu\text{dyne}/\text{cm}^2$ )	$2 \times 10^5$	$2 \times 10^5$	$3 \times 10^5$
$C_{\text{O}_2, \text{Out}}$ ( $\text{mol}/\text{m}^3$ )	0.219	0.219	0.219

Each bioreactor had a hold-up volume of 61.5mL and the simulations were performed for 55 $\mu\text{m}$  pore size







### 3.3.7 Effect of Permeability on Pressure Drop

During tissue regenerative process, cells proliferate, scaffold degrades, and extracellular matrix deposition takes place. These transient processes alter the permeability of the scaffold, eventually decreasing its value to the level of mature tissue that would be replaced in the body. To understand the implications of these dynamic changes, simulations were carried out altering the permeability in the Brinkman equation. To provide a physical nature of the reduction in permeability, different pore sizes were assumed while not changing the number of pores. Similar to our previous report (Lawrence, Devarapalli et al. 2009), the pressure drop increased with reduced permeability. The pressure drop was inversely proportional to  $1/k$  as predicted by the Brinkman equation. The permeability changed along with the pore size (**Table 3.10**). The process of tissue regeneration would reduce the pore space available for fluid flow. Hence the pore size decreased but the number of pores per area would remain the constant. Hence, to understand these dynamic changes, simulations were carried out with different pore sizes ranging from 25  $\mu\text{m}$  to 75  $\mu\text{m}$  at nutrient medium flow rate of 25 mL/min and constant number of pores per unit area of 318 pores/ $\text{mm}^2$  (Podichetty 2009). The **Table 3.11** shows the effect of permeability on pressure drop.

**Table 3.10 Effect of Pore Size on Permeability**

Pore Size( $\mu\text{m}$ )	Permeability( $\times 10^{-14} \text{m}^2$ )
25	305
50	4878
75	24700

**Table 3.11 Effect of Permeability on Pressure Drop**

Pore Size( $\mu\text{m}$ )	25	50	75
No. of nodes	400781	400781	400781
$\Delta P(\text{Pa})$ Profile			
			
$\Delta P(\text{Pa})$	69.3	4.68	1.21
$\tau(\mu\text{dyne}/\text{Cm}^2)$	$0.6 \cdot 10^5$	$0.6 \cdot 10^5$	$0.6 \cdot 10^5$
$\text{C}_{\text{O}_2, \text{Out}}(\text{mol}/\text{m}^3)$	0.218	0.218	0.218

Each bioreactor had a hold-up volume of 61.5mL and the simulations were performed at a flow rate of 25mL/min

### **3.4. Summary**

Thus the bioreactor design was optimized using the simulation. It is observed that with increase in scaffold diameter, the hold-up volume increased. To reduce the hold-up volume, the semi-angle was increased. However, the resulting design had non-uniform distribution of nutrients. Hence the change in the design of the bioreactor was incorporated by adding a distributor system. This design was selected for further study and optimized as it yielded uniform nutrient distribution and shear stress. There was no significance of the change in the inlet or outlet diameter. But when the flow rate was increased, the pressure drop across the bioreactor increased. Also, when the thickness of the scaffold was increased, the outlet oxygen concentration decreased, but still was more than the minimum oxygen concentration required for the survival of the cells. The pore size was changed to study the effect of permeability and it was observed that with increase in the pore size, the pressure drop across the bioreactor decreased.

## CHAPTER IV

### EXPERIMENTAL VALIDATION

#### 4.1. Introduction

In the previous chapter, various design features of the axial-flow bioreactor were studied. From these simulations, a high-aspect ratio bioreactor configuration with distributor system shown in **Figure3.2(c)** was suggested to be suitable for culturing cells. In order to understand the utility of the simulation, experimental validation of the methodology and nutrient distribution is necessary. A bioreactor prototype was constructed for experimental studies. Scaffolds of chitosan gelatin were fabricated using Controlled Rate Freezing and Lyophilization Technique (CRFLT). Using the bioreactor and the scaffold, experiments were performed at same flow rates as in the simulation studies to measure the pressure drop across the bioreactor. In addition, to understand the nutrient distribution in the bioreactor residence time distribution analysis using step input technique was performed.

## 4.2 Materials and Methods

### 4.2.1. Bioreactor Construction

Bioreactor was manufactured using biocompatible polycarbonate polymers (Mathur, Collier et al. 1997). For the purpose of loading the scaffold and the cells, bioreactor assembly was split into two pieces (**Figure 4.1**):

- i) top piece containing the conical structure and outlet and
- ii) bottom piece containing the inlet and the distributor system.

Both pieces were attached using stainless steel screws and they house a cavity which is used for placing the Teflon sheet and the scaffold.

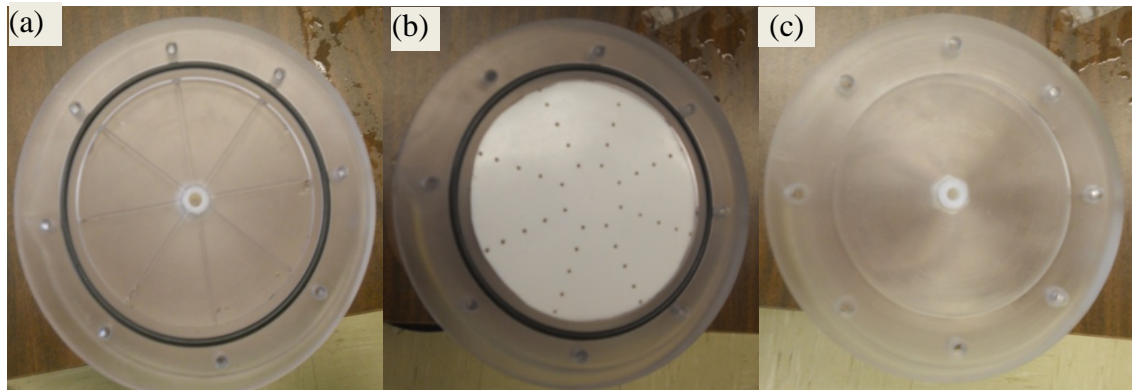


**Figure 4.1. Constructed Bioreactor Pieces. (a) Bottom piece of the reactor showing the distributor system, (b) Teflon sheet with sprinklers placed on the distributor system, and (c) Top piece of the reactor showing the conical section.**

### 4.2.2. Preparation of the Porous Scaffold

Chitosan with 190-310 kDa MW and 85% degree of deacetylation, Gelatin Type-A (Bloom 300), and glacial acetic acid were obtained from Sigma Aldrich (St. Louis, MO). Ethanol (200 proof) was obtained from Aaper Alcohol and Chemical Company (Shelbyville, KY).

Chitosan-gelatin solution was prepared in 0.1M acetic acid using deionized water. Scaffolds were fabricated using CRFLT (**Figure 4.2**), following a methodology extensively used in our laboratory (Madhally and Matthew 1999; Moshfeghian, Tillman et al. 2006). In brief, a well of known diameter was prepared on Teflon sheet using silicon glue and the chitosan-gelatin solution was poured in the well and was frozen at -80°C overnight. On top of the frozen solution, a wet paper towel was placed to remove the skinny layer and the assembly was refrozen. Prior to lyophilization (or sublimation), paper towel containing the skinny layer was peeled off. Frozen solutions were lyophilized overnight using bench top Virtis freeze dryer (Gardiner, NY). Removal of ice by sublimation resulted in pores resembling the shape of ice.

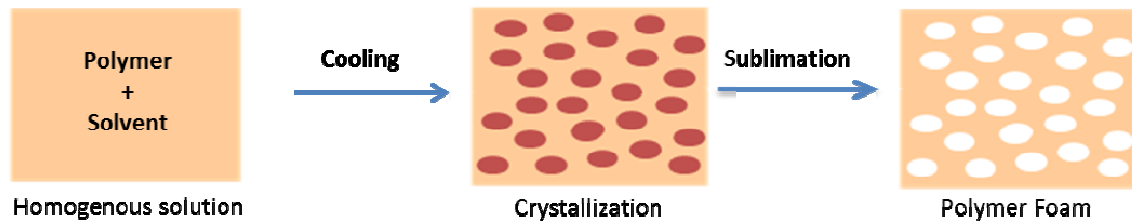


**Figure 4.2. Schematic of the CRFLT Process used in Scaffold Generation.**

Prior to using these scaffolds, acetic acid remaining in the scaffold has to be removed. For this purpose, dried samples were first incubated with pure ethanol for ten minutes and washed four times with phosphate buffered saline (PBS).

#### **4.2.3. Validating Pressure Drop**

Experiments were performed to measure the pressure drop at flow rates used in simulation studies, in order to validate the governing equations used in the simulation. Experimental set up consisted of a fluid reservoir, a variable speed Masterflex L/S

peristaltic pump, an in-line physiological pressure transducer (Capto SP844, Capto, and Skoppum, Norway), the in-house fabricated bioreactor and a waste container (**Figure4.3**). The pressure transducer was connected to a computer via Powerlab/4SP System (ADI Instruments, Inc., Colorado Springs, CO) and data were acquired using Chart™ 5 for Windows. In all experiments, averaged voltage values for 1 minute duration were recorded. A correlation was developed between voltage measured and the corresponding pressure drop, with the help of a manometer (Podichetty 2009). From three replicate experiments, average calibration was found to be:

$$\text{Pressure (in Pa)} = 4287.3 * \text{Voltage (in mV)} + 6512.6.$$

This relationship was used in all pressure drop determination experiments. Peristaltic pump was also calibrated for the tubing size by determining the flow rate to the settings on the pump. The volumetric flow rate was determined by collecting the volume of water in one minute using a measuring jar. A calibration was developed between the pump setting to the actual flow rate, which was used while setting various flow rates.

Experiments were conducted at flow rates of 5,10,15,20 and 25 mL/min. After allowing the bioreactor to achieve a steady voltage, voltage readings were measured. Experiments were performed in the following three conditions:

*i) without bioreactor*-the bioreactor was removed from the flow system and the tubes were connected to measure the pressure drop without the bioreactor. Each time the pressure reading was subtracted from the pressure drop value at zero flow rates. This difference gave the pressure drop due to fittings and tubing in the flow system without the bioreactor.

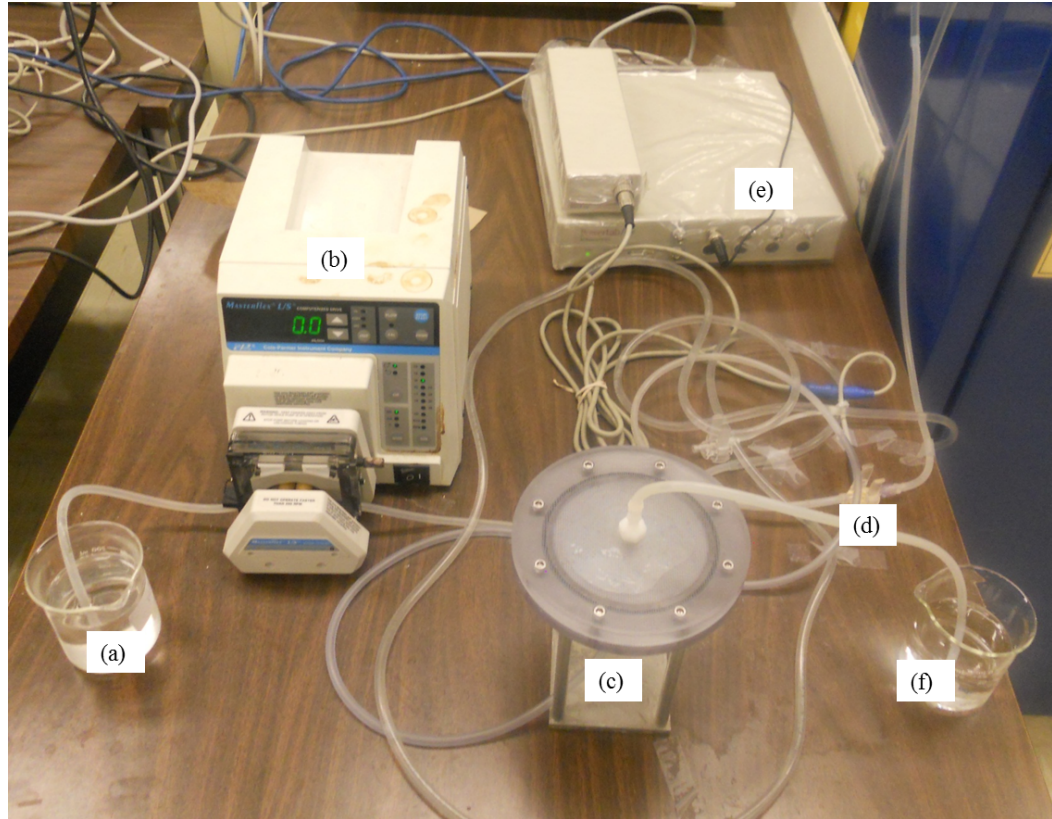


**Figure 4.3. Experimental Setup to Measure Pressure Drop across the Bioreactor. (a) Feed, (b) Pump, (c) Bioreactor, (d) Pressure transducer, (e) Powerlab, (f) Outlet**

*ii) with the bioreactor and without scaffold-* the bioreactor was placed in the flow system without the scaffold and the pressure drop was measured. Again, each pressure reading was subtracted from the pressure drop at zero flow rate. To determine the pressure drop due to the bioreactor alone (i.e., without the scaffold), pressure drop from the experiments without the bioreactor were subtracted.

*iii) with the bioreactor and 2%-2% chitosan-gelatin scaffolds -* the scaffold was placed inside the bioreactor and the pressure drop was measured. Then pressure drop was subtracted from the value measured at zero flow rate. To determine the pressure drop due to the bioreactor and scaffold, pressure drop from the experiments without the reactor were subtracted.



#### 4.2.4 Residence Time Distribution Analysis

The flow system used to measure the pressure drop was modified (**Figure 4.4**) to introduce a tracer in the step input mode, similar to a previous publication (Lawrence, Devarapalli et al. 2009). In brief, the tubing system was designed in order to include two fluid reservoirs and two waste containers. Two separate tubes were passed through the peristaltic pump, one from a water reservoir and another from a reservoir filled with tracer solution.

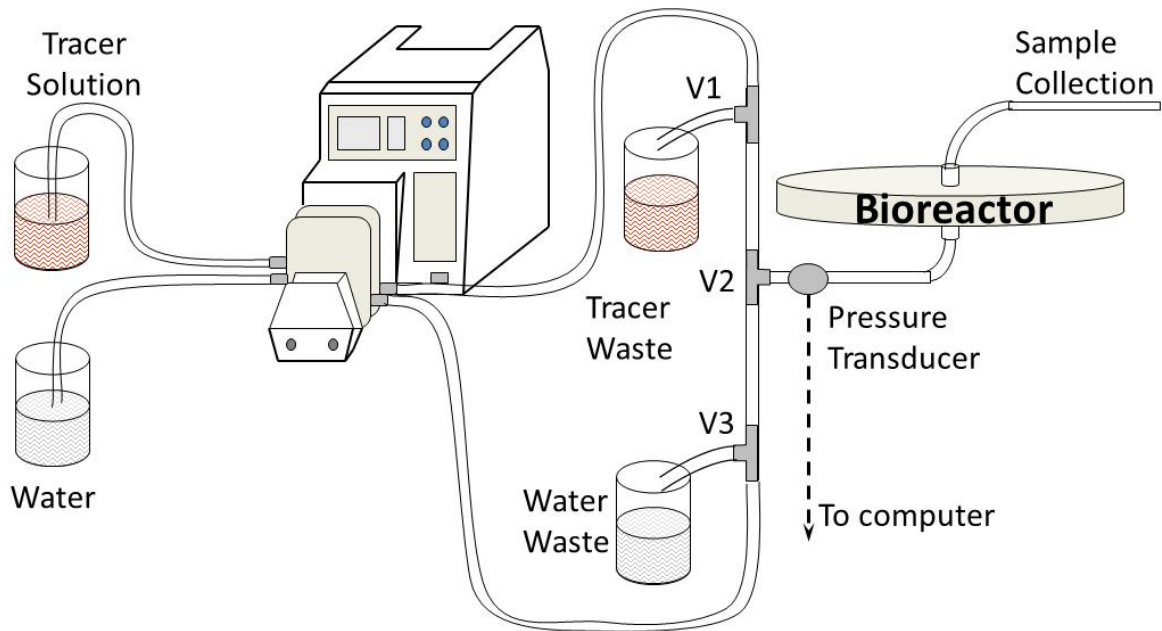


**Figure 4.4. Schematic of the Perfusion System to Assess the Residence Time**

**Distribution in the Bioreactor (Original source: (Devarapalli 2008))**

These tubes were connected using 2 three way stopcocks (V1 and V3) that diverted the fluid either towards the bioreactor or into a waste container. The two sides were connected using a three way stopcock (V2), allowing dye solution or water to enter the bioreactor.

The following steps were used to measure the mean residence time,  $t_m$  of the bioreactor:

Step 1: The flow system was primed with the valve positions V1 to dye waste and V3 to bioreactor to circulate water through the bioreactor. Water was run through the system until steady state was obtained. Once the steady state of water was reached, tracer solution was introduced into the bioreactor, by changing the position of V1 and V3 simultaneously: V1 was opened to the bioreactor and V3 was diverted to water waste container. Upon introduction of the tracer, 0.5 to 1 mL samples were collected at various times until 4 times the space time (from rule of thumb, three to four times the space time was the transient time needed for steady state).

Step 2: One hundred micro liter of sample from each time point was dispensed in to a 96-well plate. Based on the initial spectral scan of the tracer solution, absorbance was measured at 490 nm using Spectramax Emax spectrometer (Molecular Devices, Sunnyvale, CA). Absorbance of the original tracer solution ( $A_0$ ) was measured and  $A(t)/A_0$  was calculated. Based on Beer's Law, the relative concentration  $C(t)/C_0$  was calculated from equation 4.1

$$\frac{C(t)}{C_0} = \frac{A(t)}{A_0} \quad (4.1)$$

Step 3: Using Sigma Plot 12 (SPSS Science, Chicago, IL),  $C(t)/C_0$  was plotted for various time points. Based on the curve characteristics, Chapman 3-parameter equation (4.2) was selected to fit the data points

$$\frac{C(t)}{C_0} = a(1 - e^{-bt})^c \quad (4.2)$$

where a, b and c are the constants, which were determined by fitting the experimentally obtained  $C/C_0$  vs t curve.

Step 4: The residence time distribution function,  $E(t)$ , for a positive step change in the tracer concentration was calculated using the equation (Fogler 2006)

$$E(t) = \frac{d}{dt} \left[ \frac{C_{mix}(t)}{C_0} \right]_{Step} \quad (4.3)$$

For this purpose, Chapman 3-parameter equation was differentiated w.r.t time and used to calculate  $E(t)$  at various time steps.

Step5: Mean residence time was calculated using the equation 4.4

$$t_{mean} = \frac{\int_0^{\infty} tE(t)dt}{\int_0^{\infty} E(t)dt} \quad (4.4)$$

For this purpose,  $tE(t)$  was calculated at different time intervals and integrated numerically to find the area under the curve. Further,  $E(t)dt$  was also integrated for the experimental duration. Although the denominator in Eq.(4.4) should equal to 1 for infinite time, but it was less than 1 in all experiments for experimental duration. Hence the numerator was divided by the denominator value to obtain  $t_{mean}$ .

Experiments were repeated three times for each condition and analyses were performed individually to determine  $t_{mean}$ . The average values were calculated along with the standard deviations. Significant differences between two groups were evaluated using a one way analysis of variance (ANOVA) with 99% confidence interval. When  $p < 0.05$ , differences were considered to be statistically significant.

## 4.3 Results and Discussion

### 4.3.1 Pressure Drop Comparison

While performing CFD simulations, various assumptions were used including the calculation of permeability using cylindrical pores for chitosan-gelatin scaffolds prepared by freezing at -80 °C. Hence, validating the simulation results with experimental results was necessary. For this purpose, scaffolds were prepared at identical conditions and pressure drop was measured experimentally at various flow rates. The pressure drop values obtained from the experiment were compared (**Figure 4.5**) with those from simulation to validate the governing equations used in the simulation. The pressure drop values recorded in each step are shown in **Tables B.1 -B.4** in **Appendix B**. These results indicated less deviation in pressure drop for the bioreactor without the scaffold between the simulation and experimental results. In the presence of the scaffold, the pressure drop increased linearly with flow rate. When the scaffold was present, the fluid passed through the porous medium which resulted in increased pressure drop.

Experimentally determined pressure drop values with the scaffolds were approximately double the simulation values at all flow rates. Since the pressure drop is inversely proportional to the scaffold permeability in the Brinkman's equation (Equation 3.3), it was suspected that this deviation was due to reduced permeability. One possibility is that incomplete removal of the skinny layer in the scaffold could increase the resistance to flow by decreasing the number of open pores that allow fluid flow. To understand this possibility, simulations were performed at different flow rates using half the value of the original permeability. These simulation results agreed with the experimental results suggesting the possibility of reduced permeability due to skinny layer.

Another possibility is that the permeability value calculations Kozeny equation based on cylindrical pores oriented in the direction of flow may not be appropriate. This is possible as the same assumption was valid in flow-through bioreactor. Hence evaluating the permeability with the assumption of pores aligned perpendicular to the flow direction is necessary. Curvatures within each pore could increase the resistance to flow.

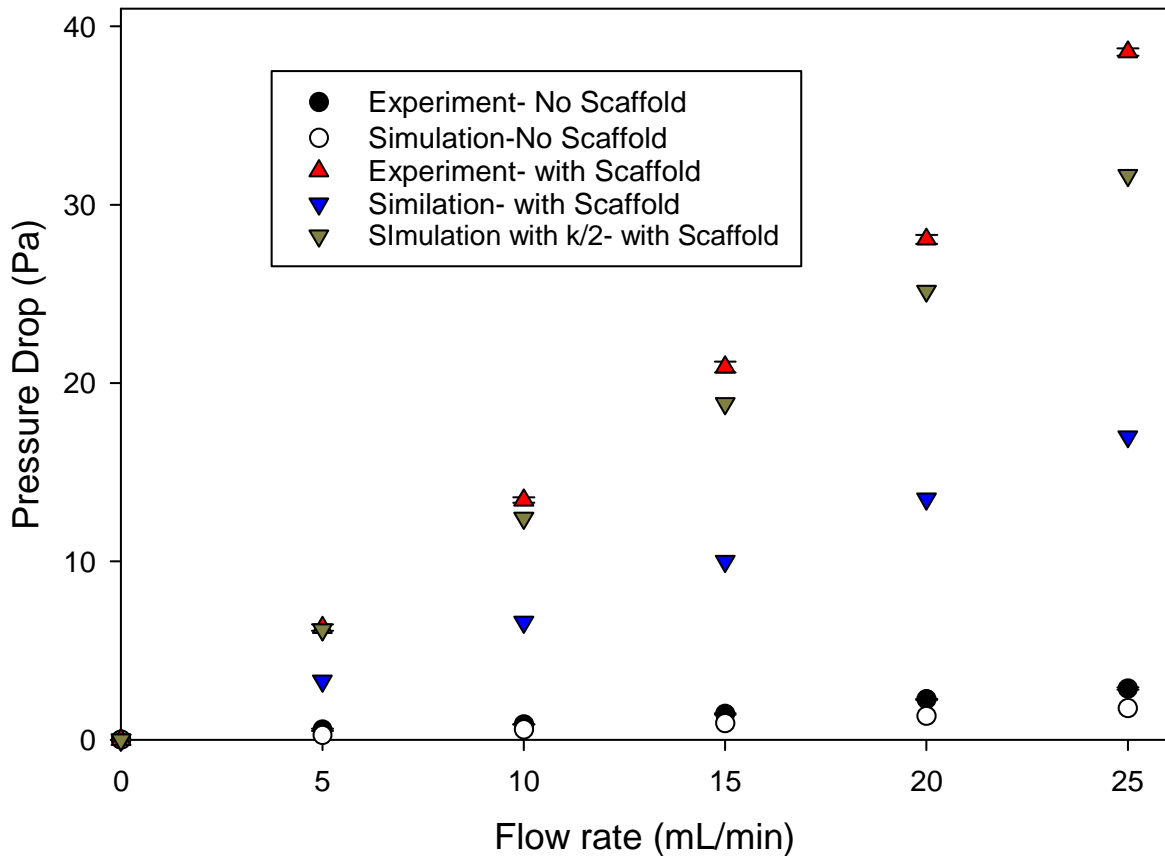


**Figure 4.5 Experimental Validation of Pressure Drop (Pa) vs. Flow Rate (mL/min)**

#### 4.3.2 Residence Time Distribution

One of the requirements of bioreactors is uniform distribution of nutrients in the entire scaffold area. Residence time distribution (RTD) analysis is used to measure the dispersal of a molecule in a flowing medium owing to the combined action of a velocity

profile and molecular diffusion. The RTD experiments were performed in the axial-flow bioreactor to understand the distribution of nutrients. A red colored food-dye tracer was used to determine the nutrient mean residence time in the bioreactor with three set of conditions, i) bioreactor without the scaffold and without the distributor, ii) bioreactor without the scaffold and with the distributor and iii) bioreactor with the scaffold and with the distributor.

The changes in the tracer concentration at the bioreactor outlet were plotted for various time periods (**Figures 4.6**). The **Tables B.5, B.6 and B.7** in **Appendix B** shows the values recorded experimentally. The results showed that during bioreactor operation without the distributor and without the scaffold, the tracer exited the bioreactor sooner compared to other cases.

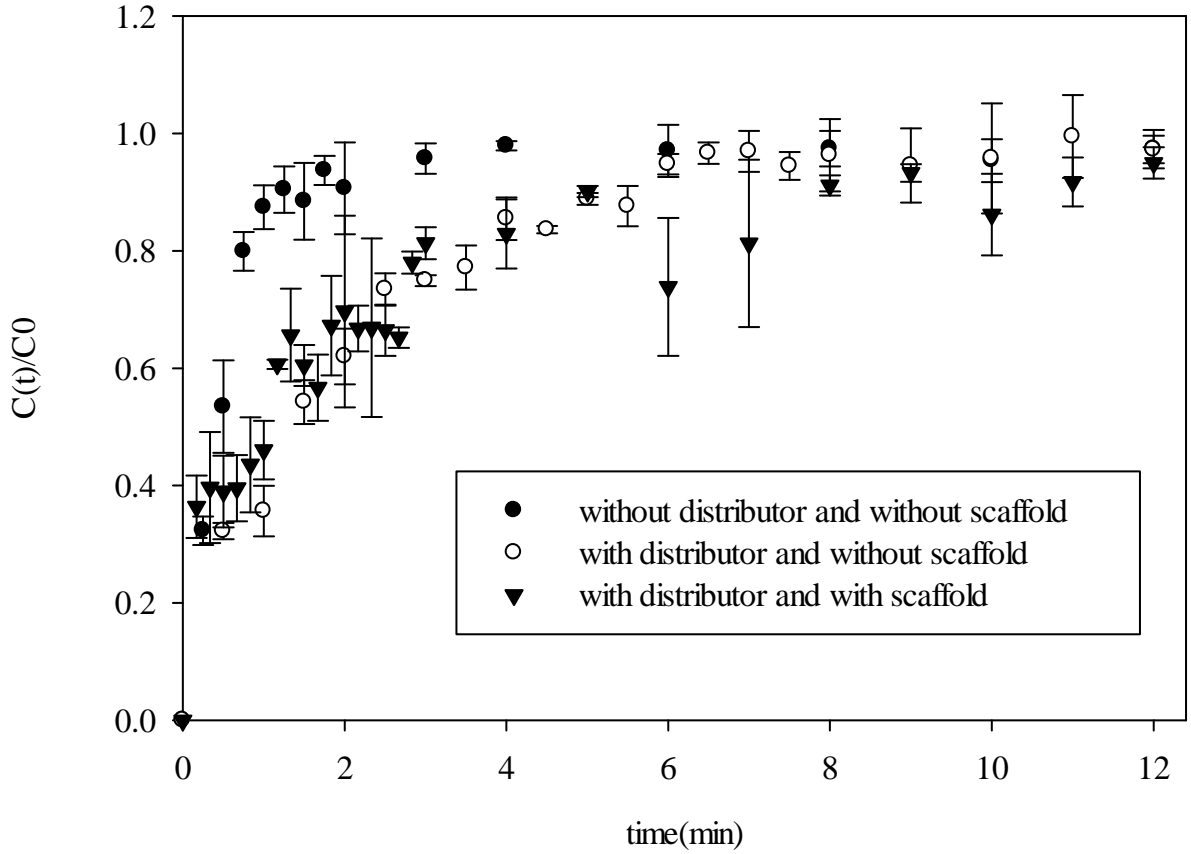


**Figure 4.6. Transient Changes in the Concentration of the Tracer at the Outlet of the Axial Flow Bioreactor**

When distributor alone was present without the scaffold, the tracer took longer time to exit the bioreactor, even compared to with the scaffold operation. However, incorporating the scaffold into the bioreactor reduces the free volume of the bioreactor which results in reduced residence time; free volume is the space available for fluid flow i.e., subtracting the volume occupied by the scaffold biomaterial and the distributor. This could be the reason for observed difference between with and without the scaffold results. Next,  $E(t)$  was calculated for different time steps and plotted as a function of time (**Figures 4.7**). The  $E(t)$  peak heights for the case when the bioreactor was operated without the distributor and without the scaffold (case 1) and when the bioreactor was

operated with the distributor and with the scaffold (case 3) were higher than for the case when the bioreactor was operated with the distributor and without the scaffold (case 2).

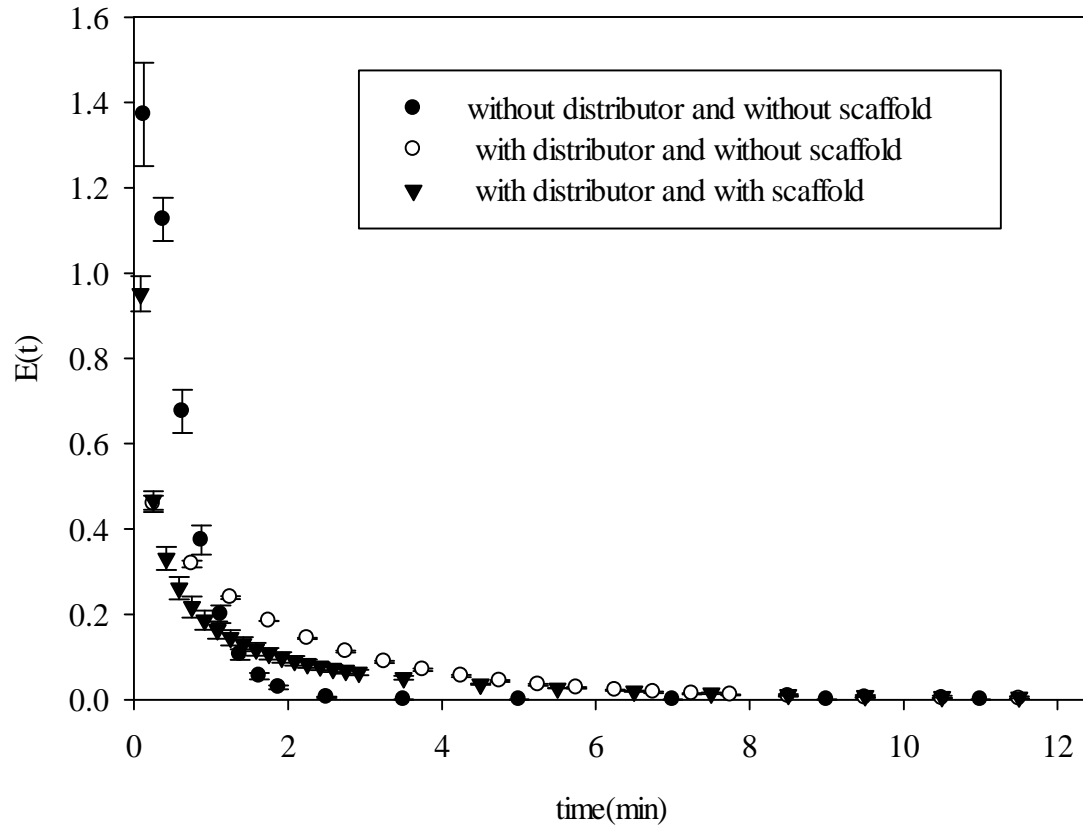


**Figure 4.7E-curve for the Axial Flow Bioreactor**

Additionally, peak spreading was observed in case 1, case 2, and case 3 indicating dispersion of the tracer or flow non-idealities. These observations suggest that there are dead-spaces within the bioreactor.

To understand the distribution of nutrients,  $tE(t)$  curve (**Figures 4.8**) was plotted from which  $t_m$  was calculated. The  $t_m$  for the bioreactor without distributor and without scaffold was  $(29 \pm 1.9)$  s, which was significantly smaller than the bioreactor with distributor and without scaffold  $(114.6 \pm 5.3)$  s. This could be attributed to channeling without distribution as observed in the simulation. Some axial flow bioreactors which



have not used distributor or entrance cone to facilitate nutrient distribution may be subjected to similar effects(Bancroft GN 2003). Hence,

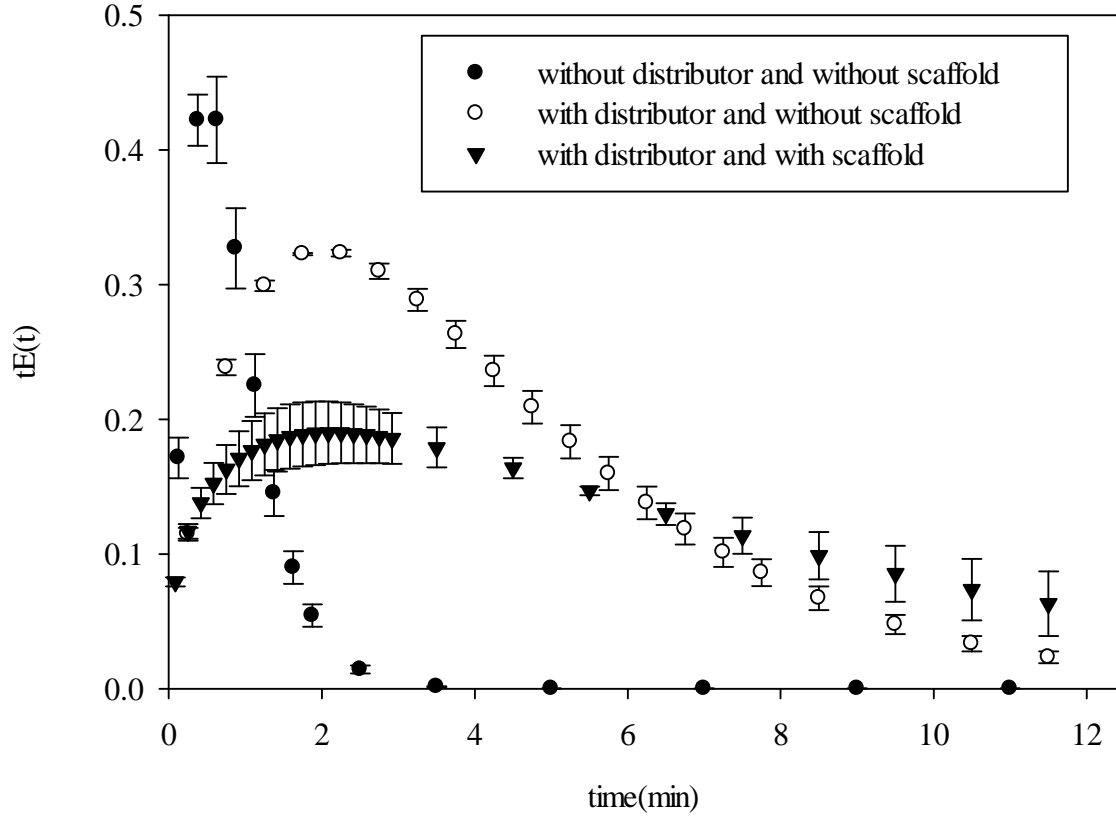


**Figure 4.8 tE(t) vs t Curve**

incorporation of a distributor is essential to disperse the nutrients. When scaffold was introduced into the bioreactor,  $t_m$  decreased marginally ( $109.8 \pm 12s$ ) attributed to decreased free volume.

To compare the deviations in the distribution of nutrients from ideal conditions, space time was calculated using free volume of the reactor (**Table 4.1**) for a volumetric flow rate of 15mL/min. The  $t_m$  for the bioreactor without distributor and without scaffold obtained experimentally was 6 times less than the calculated value. This implies that the fluid distribution was limited to only 15% volume in the central region. Incorporation of

the distributor into the bioreactor distributed the nutrients to nearly 70% of the bioreactor, suggesting significant improvement in the nutrient distribution.

**Table 4.1. Comparison of Residence Time Distributions**

Bioreactor type	Free Volume (mL)	Mean residence time, $t_m$ (min)		Distributed Volume (mL)	Dead Volume (mL)
		Theoretical	Experimental		
Without distributor and without scaffold	48	3.2	0.48	7.2	40.8
With distributor and without scaffold	41	2.73	1.91	28.65	12.35
With distributor and with scaffold	37	2.47	1.83	26.4	9.6

Presence of scaffolds also showed similar distribution. From the simulation results, it could be suggested that additional holes can be incorporated into the distributor where low oxygen concentration is observed (**Figure 3.2(f)**). One could connect annular channels into the bottom piece of the bioreactor near the periphery of the cylinder.

## CHAPTER V

### CONCLUSION AND RECOMMENDATIONS

#### 5.1 Conclusion

The axial-flow bioreactor developed had several advantages than the currently available ones. However, various geometric factors affecting the distribution of nutrients in axial-flow bioreactor for use in tissue regeneration are not well understood. The current study evaluated the influence of various factors on nutrient distribution in axial-flow bioreactors with an ability to accommodate high aspect ratio tissues. The following are the conclusions based on the two specified aims::

##### **Specific Aim 1: Optimization of Bioreactor via CFD Simulation**

- i) When the diameter of the bioreactor was scaled up from  $x$  to  $5x$  mm the hold-up volume of the bioreactor increased from 4.66 mL to 319 mL. However, the nutrient distribution was similar..
- ii) When the semi-angle of the cone was increased for the  $5x$  mm diameter bioreactor from  $sa^\circ$  to  $2.67 sa^\circ$ , the volume of the bioreactor decreased drastically. This also affected the nutrient distribution, particularly at the periphery of the scaffold.
- iii) When the distribution system was incorporated in the region immediately.

below the scaffold, nutrient distribution increased to larger regions of the scaffold.

- iv) Changing the inlet diameter or the outlet diameter while keeping all other configurations constant had no effect on the hydrodynamic characteristics and the nutrient distribution.
- v) When the thickness of the scaffold was increased from  $z$  to  $3z$  mm with constant cell density, pressure drop increased. Further, the outlet concentration of oxygen decreased marginally. However, the outlet oxygen concentration was still higher suggesting the possibility of growing thicker tissues using axial-flow bioreactors.
- vi) When the flow rate was increased from 5 mL/min to 25 mL/min the pressure drop across the bioreactor increased from 10 Pa to 17 Pa. To understand the changes in nutrient transport during tissue regenerative process where the pore sizes could decrease, the pore size was decreased from 75  $\mu\text{m}$  to 25  $\mu\text{m}$ . During this time, the pressure drop across the bioreactor decreased from 69.3 Pa to 1.21 Pa but there was sufficient oxygen for the growth of cells.

### **Specific Aim 2: Validation of the Simulation Results with the Experiments**

- i) When the flow rate was increased from 5 mL/min to 25 mL/min the experimental pressure drop for the bioreactor without the scaffold increased from 0.5 Pa to 2.8 Pa. Pressure drop obtained from the simulation for the bioreactor without the scaffold increased from 0.26 to 1.76 Pa for the same change in the flow rate. Hence the experimental results validated the

simulation of the bioreactor in the non-porous region. When the experiments were conducted for the bioreactor with the scaffold the pressure drop across the bioreactor increased from 6.3 Pa to 38.6 Pa, whereas the simulation pressure drop increased from 6.2 to 17.0Pa. The reason for the deviation in the pressure drop at higher flow rates was attributed to the skinny layer in the top region of the scaffold. Hence, when the simulation was performed with half the value of the initial permeability used, the pressure drop increased from 6.2 Pa to 31.7 Pa.

- ii) Dead volume obtained from the RTD analysis for the bioreactor i) without the distributor and without the scaffold was 40.8 mL ,and ii) with the distributor and with the scaffold was 9.6 mL. Experiments suggesting this decrease in the dead volume with the addition of the distribution system validate the simulation results.

## **5.2 Recommendations**

The future recommendations of the study can be:

Improvement in distribution system: Current distributor system increased the nutrient distribution to nearly 70% of the bioreactor. However, additional distributor systems have to be evaluated to ensure nutrient distribution in the entire region of the scaffold. For example, the distributor systems in the form of annulus near the periphery of the scaffold could be implemented to improve the nutrient distribution and thereby reduce the dead volume of the bioreactor. However, simulations have to be performed to confirm these possibilities.

Asymmetrical openings in the Teflon sheet over the distributor section i.e., smaller diameter distributors near the center and larger diameter distributors towards the periphery of the bioreactor to make sure that the shear stress and the nutrient distribution is uniform throughout the region of the scaffold.

Experimental Validation of bioreactors: In this study, RTD studies were performed using the scaffolds. However, to understand the utility of the bioreactor and to validate the nutrient distribution with consumption, cell culture studies have to be performed. One has to seed the same number of cells and measure the outlet oxygen concentration as well glucose concentration.

Pressure drop studies showed difference between the experimentation and simulation.

These could be attributed to the presence of skinny layer. Further experiments are necessary where skinny layer is completely removed and then pressure drop across the bioreactor is determined experimentally matches with the simulation results. However, if there is a discrepancy between simulation and experimental results exists, this would suggest modification in the calculation of permeability. Alternative, scaffolds prepared by other techniques such as electrospinning and salt leaching could be employed to validate simulation methodology.

## REFERENCES

- (2008). "Basic principles of Tissue Engineering." from <http://textile.iitd.ac.in/highlights/fol8/01.ht>.
- Agarwal CM and R. Ray (2001). "Biodegradable polymeric scaffolds for musculoskeletal tissue engineering." Journal of Biomedical Materials Research **55**.
- Alpert E, G. A., Totary H, Kaiser N, Reich R, Sasson S. (2002a). "A natural protective mechanism against hyperglycaemia in vascular endothelial and smooth-muscle cells: role of glucose and 12-hydroxyeicosatetraenoic acid." Biochem J **362(Pt 2)**: 413-422.
- Bancroft GN, S. V., Mikos AG (2003). "Design of a flow perfusion bioreactor system for bone tissue-engineering applications." Tissue Eng **9**(3): 549-554.
- Capuani, F., D. Frenkel, et al. (2003). "Velocity fluctuations and dispersion in a simple porous medium." Physical Review E **67**(5): 056306.
- Chapekar, M. S. (2000). "Tissue engineering: challenges and opportunities " Journal of Biomedical Materials Research **53**(6): 617-620.
- Chung, T. W., J. Yang, et al. (2002). "Preparation of alginate/galactosylated chitosan scaffold for hepatocyte attachment." Biomaterials **23**(14): 2827-2834.
- Cioffi, M., F. Boschetti, et al. (2006). "Modeling evaluation of the fluid-dynamic microenvironment in tissue-engineered constructs: A micro-CT based model." Biotechnology and Bioengineering **93**(3): 500-510.
- D.L. Nettles, S.H. Elder, et al. (2002). "Potential use of chitosan as a cell scaffold material for cartilage tissue engineering." Tissue Eng **8**: 1009-1016.
- Devarapalli, M. (2008). Designing a bioreactor for regenerating high aspect ratio tissues. Masters of Science, Oklahoma State University.
- Devarapalli, M., B. J. Lawrence, et al. (2009). "Modeling nutrient consumptions in large flow-through bioreactors for tissue engineering." Biotechnology and Bioengineering **103**(5): 1003-1015.
- Dhane, D. v. (2010). Influence of diffusion in tissue engineering bioreactors. Master of Science, Oklahoma State University.
- Dvir T, B. N., Shachar M, Cohen S. (2006). "A novel perfusion bioreactor providing a homogenous milieu for tissue regeneration." Tissue Eng. **12**(10): 2843-2852.
- Fogler, H. S. (2006). Elements of chemical reaction engineering. Upper Saddle River, NJ, Prentice Hall.
- Freed, L. E., J. C. Marquis, et al. (1993). "Neocartilage formation in vitro and in vivo using cells cultured on synthetic biodegradable polymers." Journal of biomedical materials research **27**(1): 11-23.
- Freed LE, V.-N. G., Biron RJ, Eagles DB, Lesnoy DC, Barlow SK, Langer R. (1994a). "Biodegradable polymer scaffolds for tissue engineering." Bio/Technology **12**: 689-693.
- Freyman T M, Y. IV, et al. (2001). "Cellular materials as porous scaffolds for tissue engineering." Progress in Materials Science **46**: 273-282.
- Fricke, H. (1924). "A Mathematical Treatment of the Electric Conductivity and Capacity of Disperse Systems I. The Electric Conductivity of a Suspension of Homogeneous Spheroids." Physical Review **24**(5): 575-587.
- Griffith, L. G. and G. Naughton (2002). "Tissue Engineering--Current Challenges and

- Expanding Opportunities." Science **295**(5557): 1009-1014.
- Hidalgo-Bastida, L. A., S. Thirunavukkarasu, et al. (2012). "Modeling and design of optimal flow perfusion bioreactors for tissue engineering applications." Biotechnology and Bioengineering **109**(4): 1095-1099.
- Hong, J. K. and S. V. Madhally (2011). "Next Generation of Electrosprayed Fibers for Tissue Regeneration." Tissue Engineering Part B: Reviews **17**(2): 125-142.
- Huang, Y., S. Onyeri, et al. (2005). "In vitro characterization of chitosan–gelatin scaffolds for tissue engineering." Biomaterials **26**(36): 7616-7627.
- Hutmacher, D. W. and H. Singh (2008). "Computational fluid dynamics for improved bioreactor design and 3D culture." Trends Biotechnol **26**(4): 166-172.
- Ishaug SL, C. G., Miller MJ, Yasko AW, Yaszemski MJ, Mikos AG. (1997). "Bone formation by three-dimensional stromal osteoblast culture in biodegradable polymer scaffolds." Journal of Biomedical Materials Research **36**(1): 17-28.
- J. Li, J. Pan, et al. (2003). "Culture of primary rat hepatocytes within porous chitosan scaffolds." J Biomed Mater Res **67A**: 938-943.
- J.S. Mao, L. Zhao, et al. (2003). "Study of novel chitosan-gelatin artificial skin in vitro." J Biomed Mater Res A **64A**: 301-308.
- Khor, E. and L. Y. Lim (2003). "Implantable applications of chitin and chitosan." Biomaterials **24**(13): 2339-2349.
- Kim, I.-Y., S.-J. Seo, et al. (2008). "Chitosan and its derivatives for tissue engineering applications." Biotechnology Advances **26**(1): 1-21.
- Kuo CK and M. PX. (2001). "Ionically crosslinked alginate hydrogels as scaffolds for tissue engineering: part 1, structure, gelation rate and mechanical properties. ." Biomaterials **22**: 511-521
- L.J. Dortmans, A.A. Sauren, et al. (1984). "Parameter estimation using the quasi-linear viscoelastic model proposed by Fung." J Biomech Eng **106**: 198-203.
- Lawrence, B. J., M. Devarapalli, et al. (2009). "Flow dynamics in bioreactors containing tissue engineering scaffolds." Biotechnol Bioeng **102**(3): 935-947.
- LeBaron RG and A. KA (2000). "Ex-vivo synthesis of articular cartilage." Biomaterials **21**: 2575-2587.
- Leclerc, E., Y. Sakai, et al. (2004). "Microfluidic PDMS (Polydimethylsiloxane) Bioreactor for Large-Scale Culture of Hepatocytes." Biotechnology Progress **20**(3): 750-755.
- Levenspiel, O. Chemical Reaction Engineering (3rd Edition), John Wiley & Sons.
- Mackie, J. S. and P. Meares (1955). "The Diffusion of Electrolytes in a Cation-Exchange Resin Membrane. I. Theoretical." Proceedings of the Royal Society of London. Series A, Mathematical and Physical Sciences **232**(1191): 498-509.
- Mackie, J. S. and P. Meares (1955). "The Diffusion of Electrolytes in a Cation-Exchange Resin Membrane. II. Experimental." Proceedings of the Royal Society of London. Series A, Mathematical and Physical Sciences **232**(1191): 510-518.
- Madhally, S. V. and H. W. T. Matthew (1999). "Porous chitosan scaffolds for tissue engineering." Biomaterials **20**(12): 1133-1142.
- Martin, I., D. Wendt, et al. (2004). "The role of bioreactors in tissue engineering." Trends in Biotechnology **22**(2): 80-86.
- Martin, Y. and P. Vermette (2005). "Bioreactors for tissue mass culture: design, characterization, and recent advances." Biomaterials **26**(35): 7481-7503.

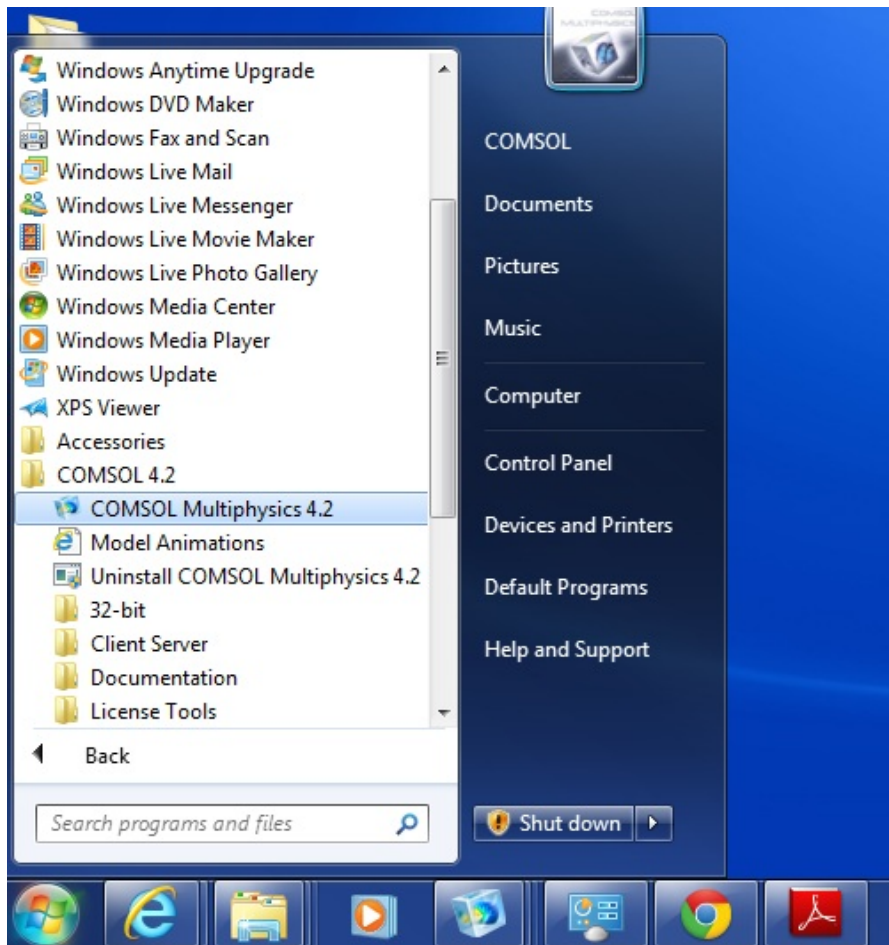


- Mathur, A. B., T. O. Collier, et al. (1997). "In vivo biocompatibility and biostability of modified polyurethanes." Journal of biomedical materials research **36**(2): 246-257.
- Maxwell, J. C. and W. Garnett (2011). An Elementary Treatise on Electricity, Cambridge University Press.
- Moshfeghian, A., J. Tillman, et al. (2006). "Characterization of emulsified chitosan-PLGA matrices formed using controlled-rate freezing and lyophilization technique." Journal of Biomedical Materials Research Part A **79A**(2): 418-430.
- Motterlini, R., H. Kerger, et al. (1998). "Depression of endothelial and smooth muscle cell oxygen consumption by endotoxin." American Journal of Physiology - Heart and Circulatory Physiology **275**(3): H776-H782.
- Pazzano, D., K. A. Mercier, et al. (2000). "Comparison of Chondrogenesis in Static and Perfused Bioreactor Culture." Biotechnology Progress **16**(5): 893-896.
- Podichetty, J. T. (2009). Effect of Fluid flow on Structural Deformation of Porous Scaffolds. Master of Science, Oklahoma State University.
- Portner, R., S. Nagel-Heyer, et al. (2005). "Bioreactor design for tissue engineering." J Biosci Bioeng **100**(3): 235-245.
- Pu, F., N. P. Rhodes, et al. (2010). "The use of flow perfusion culture and subcutaneous implantation with fibroblast-seeded PLLA-collagen 3D scaffolds for abdominal wall repair." Biomaterials **31**(15): 4330-4340.
- Ratakonda, S., U. M. Sridhar, et al. (2012). "Assessing viscoelastic properties of chitosan scaffolds and validation with cyclical tests." Acta Biomaterialia **8**(4): 1566-1575.
- Sawtell RM, D. S., Kayser MV (1995). "An in vitro investigation of the PEMA/THFMA system using chondrocyte culture." Journal of Materials Science: Materials in Medicine **6**: 676-679.
- Shigemasa, Y., K. Saito, et al. (1994). "Enzymatic degradation of chitins and partially deacetylated chitins." International Journal of Biological Macromolecules **16**(1): 43-49.
- Strain, A. J. and J. M. Neuberger (2002). "A Bioartificial Liver--State of the Art." Science **295**(5557): 1005-1009.
- Tillman, J., A. Ullm, et al. (2006). "Three-dimensional cell colonization in a sulfate rich environment." Biomaterials **27**(32): 5618-5626.
- Truskey GA, Y. F., Katz DF. (2004). Transport phenomena in Biological Systems. Upper Saddle River, NJ, Pearson Prentice Hall:317-321.
- Waggoner, R. A., F. D. Blum, et al. (1993). "Dependence of the solvent diffusion coefficient on concentration in polymer solutions." Macromolecules **26**(25): 6841-6848.
- Wendt, D., S. Riboldi, et al. (2011). Bioreactors in Tissue Engineering: Scientific Challenges and Clinical Perspectives, Springer Berlin / Heidelberg: 1-27.

## APPENDICES

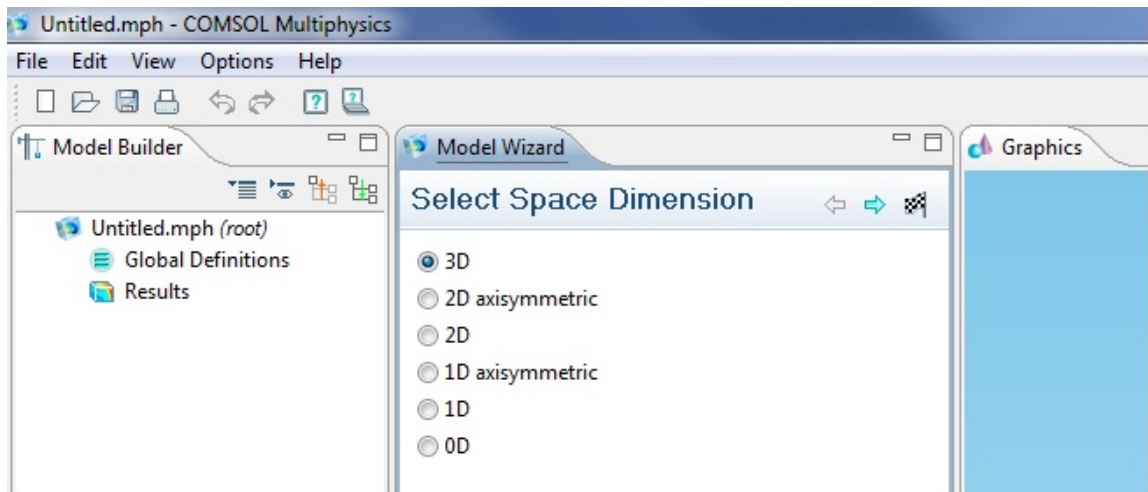
### APPENDIX A: COMSOL 4.2 Manual

1. **Start > All Programs > COMSOL 4.2>Click on COMSOL Multiphysics 4.2.**  
Model.

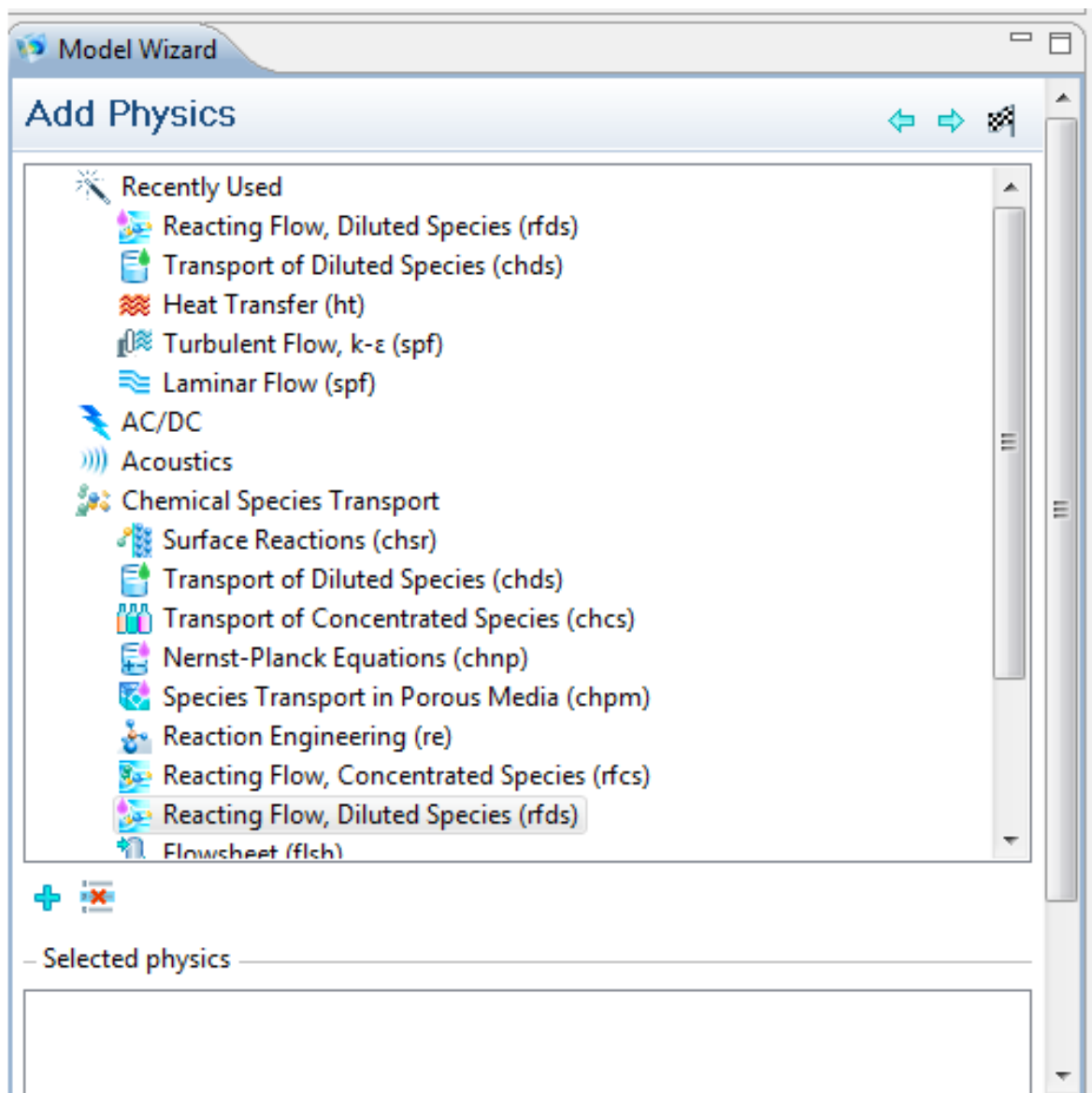


2. After opening COMSOL 4.2, the model wizard asks for the space dimension. Select 3D.

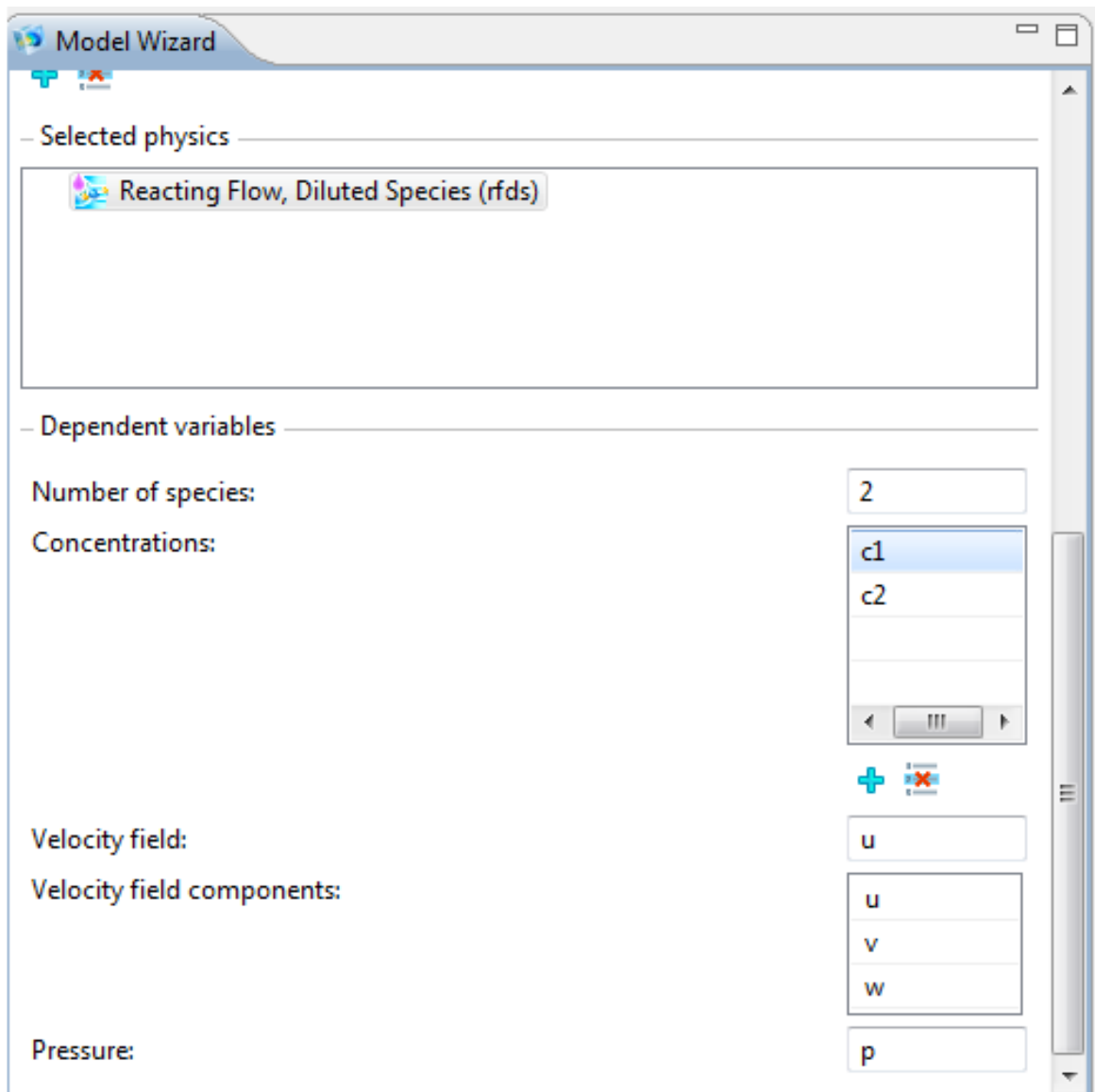
Then Click on the arrow mark above which reads Next.



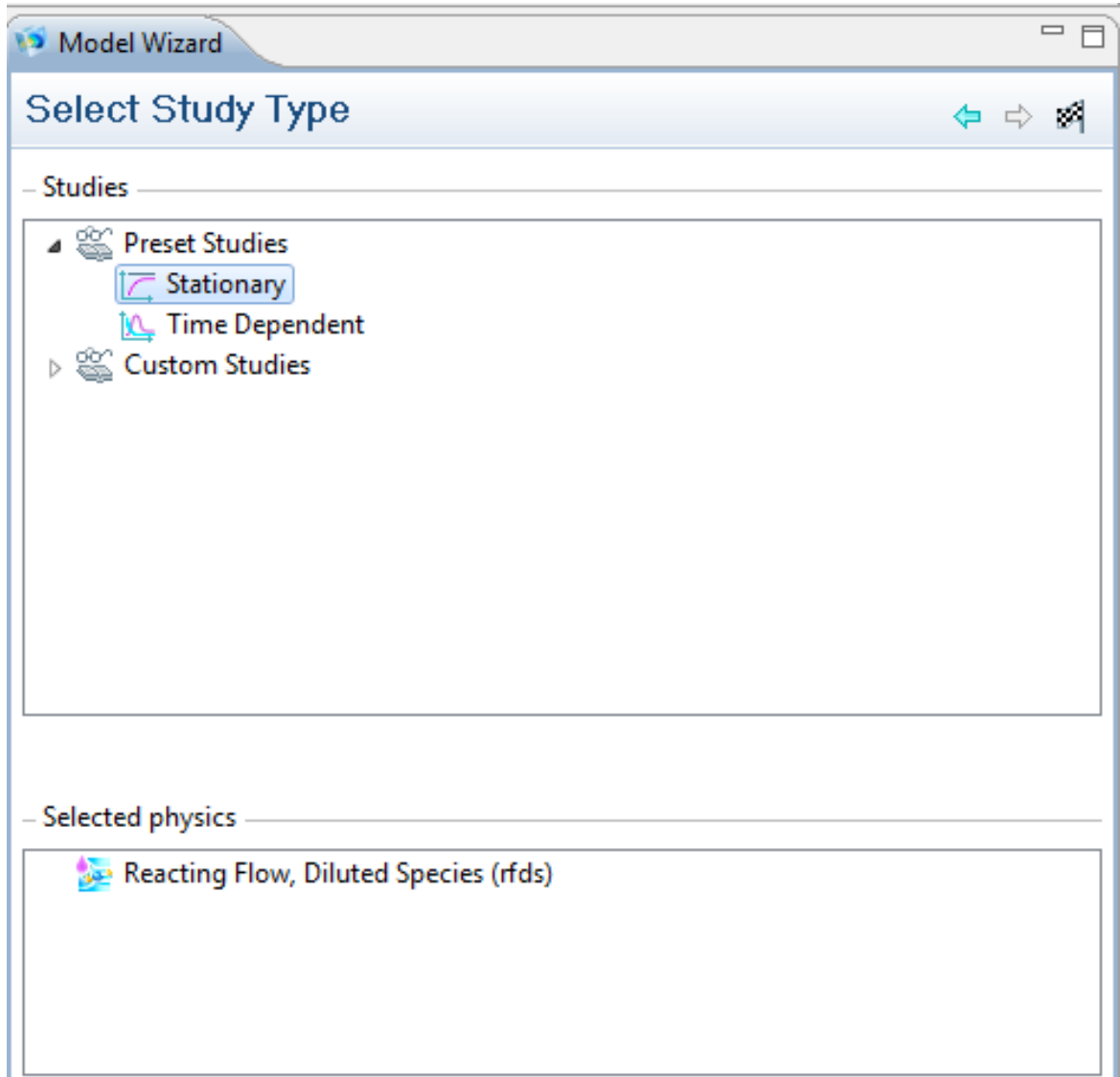
3. In the Add Physics Windows go to Chemical Species Transport>Reacting Flow, Diluted Species. Then click on the '+' button to add the selected physics.



4. In the dependent variables part of the model wizard, select the number of species as 2 and label them as c1 and c2 in the concentrations column and keep the rest as it is. Click on the 'Next' button.



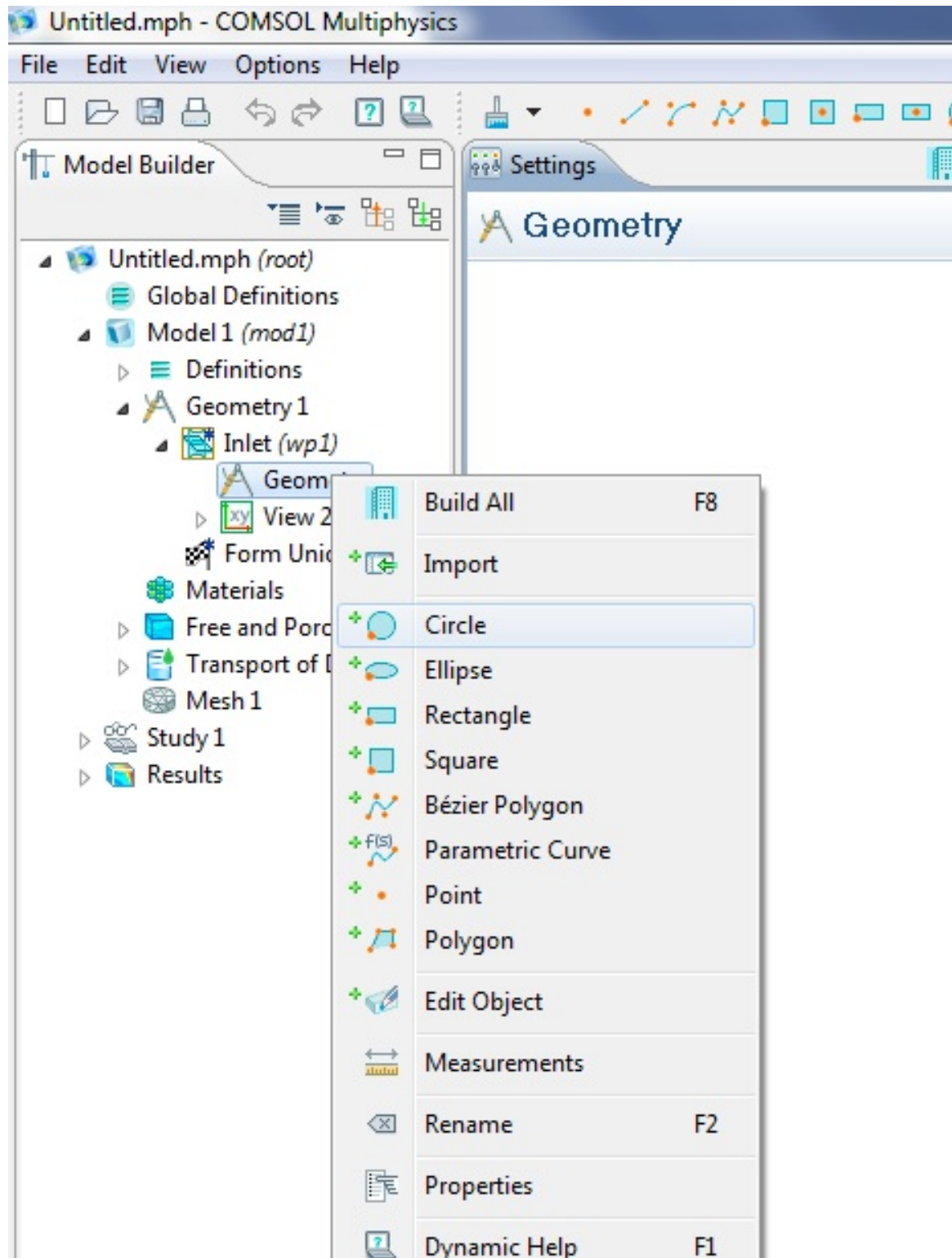
5. In the Select Study Type, Click on Stationary. Then click on Finish button located above.



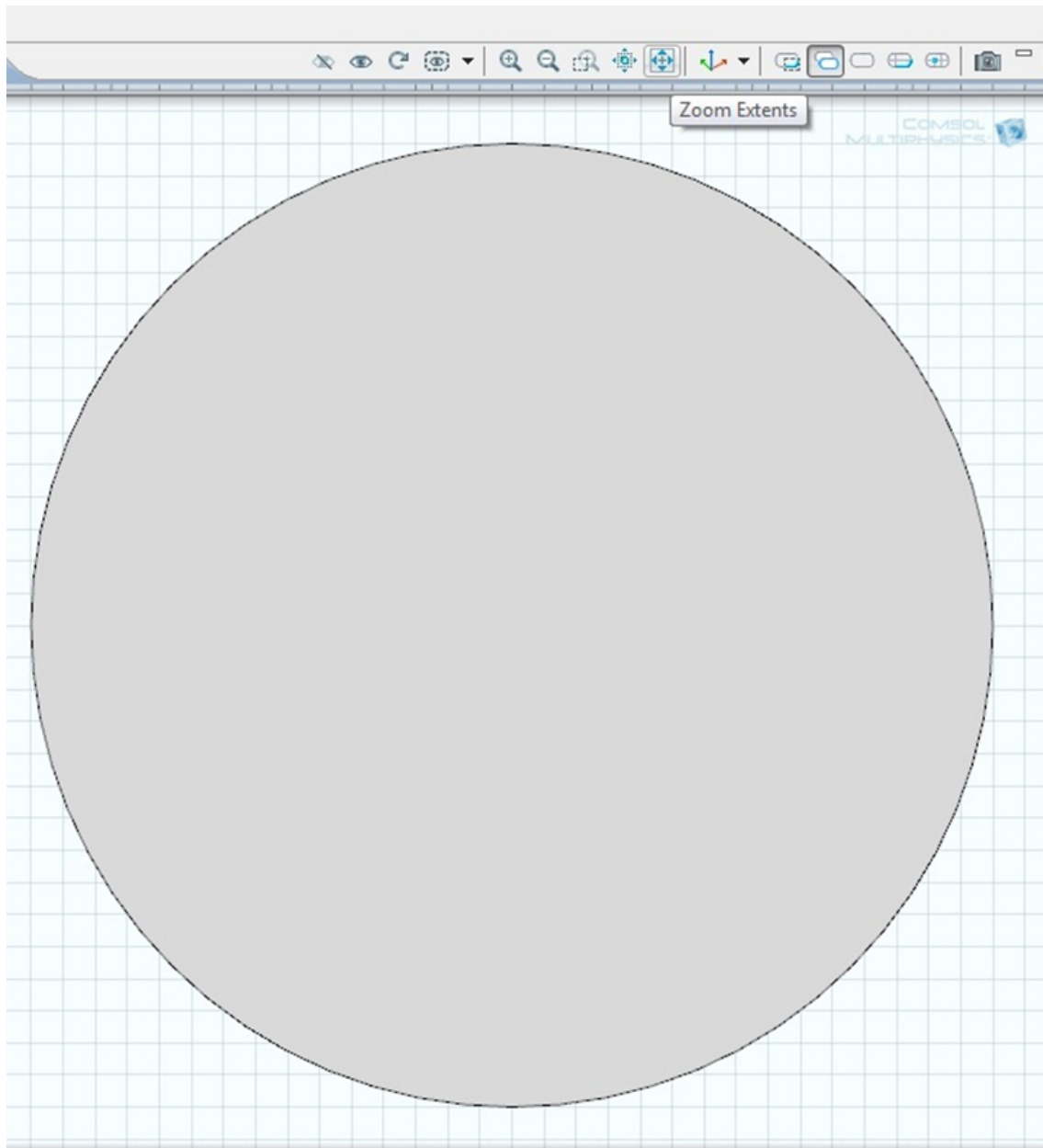
6. In the Settings window select the Length Unit as mm.

7. In the model builder window, go to model1 and right click on Geometry 1 and select Work Plane. In the setting window for work plane, select the required z-coordinate. Right click on Work Plane and rename as Inlet.

8. Next right click on Geometry located inside the work plane 'Inlet' and select Circle and edit the radius field as desired. Then Click on Build Selected button located above.

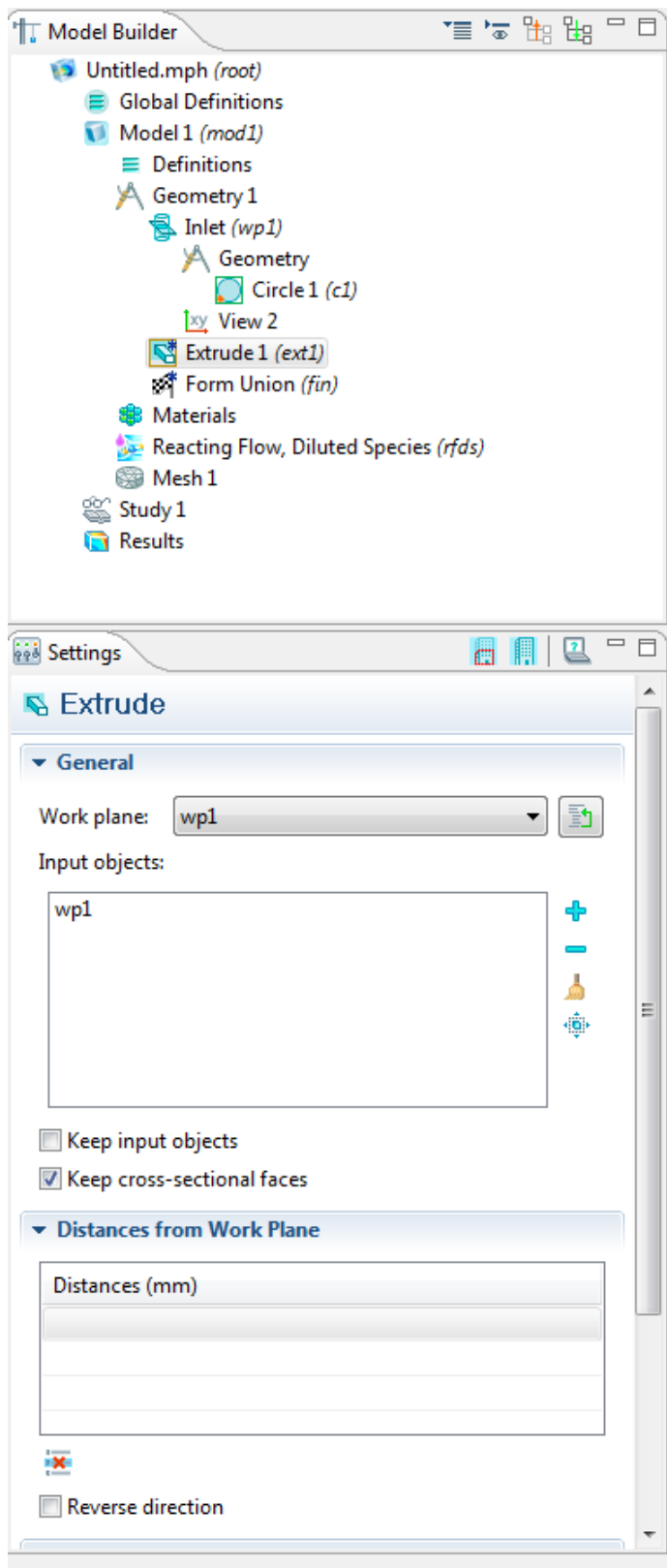


9. Then click on the Zoom Extents Button located in the graphics window.



10. Right click on Inlet in the model builder window and select Extrude. In the settings window edit the distance from Work Plane. This completes the procedure for creating a work plane and extruding it.





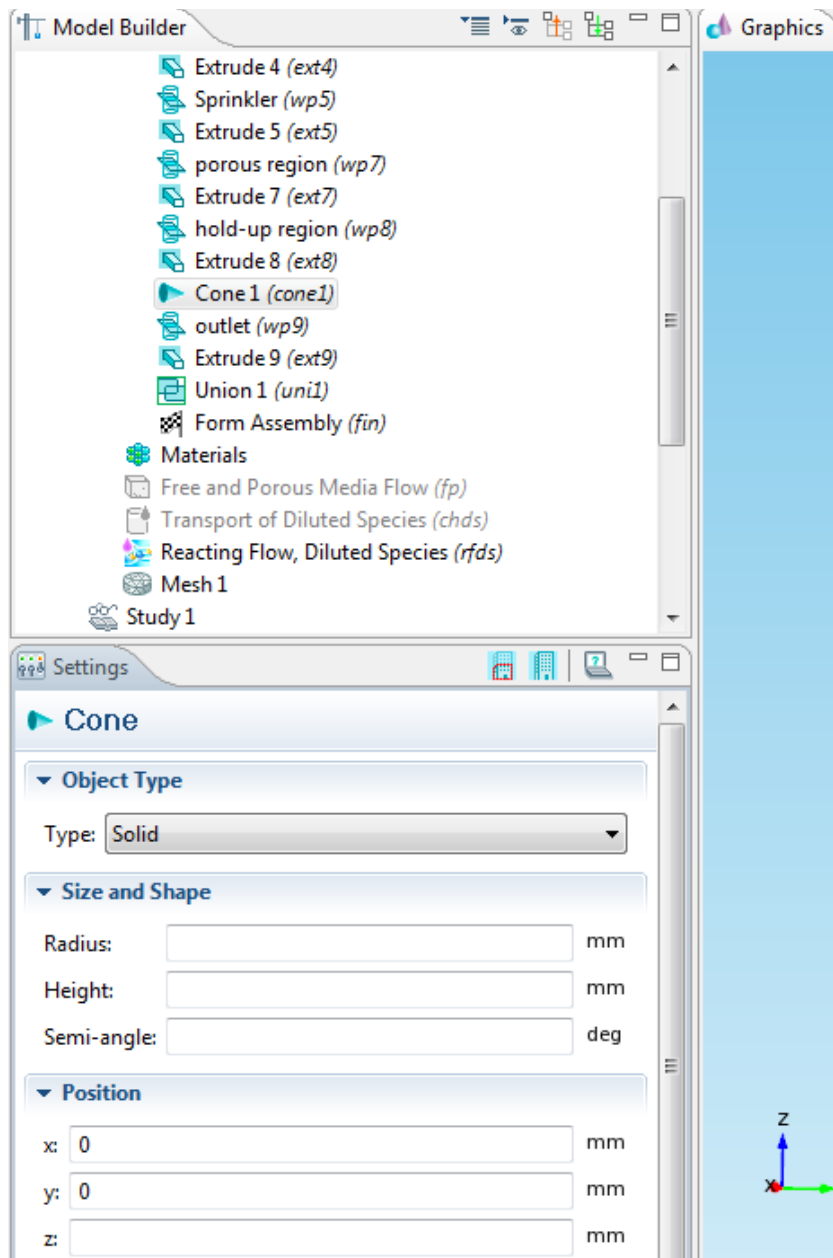
11. Now create one more Work plane and rename it as Runner. Right Click on Geometry in runner section and select Rectangle. Edit the width height sections. There are totally four rectangles in the runner section and all of these are extruded to obtain cuboid having all the three dimensions the same.

12. Next Create Work Plane and rename it as Sprinkler. This plane lies directly above the workplane 'Runner'. Forty Circles of equal radius have to be built in this work plane and then extruded.

13. Next create a work plane and rename it as Porous Region. This plane is located immediately above the 'Sprinkler' and a circle is built and extruded.

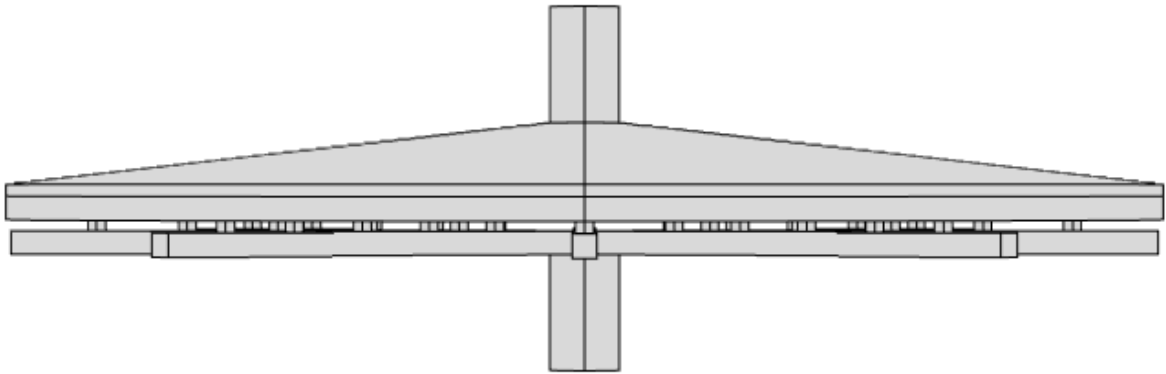
14. Create a work plane and rename it as 'Hold-up region' and choose the z-coordinate such that its workplane is located immediately above the porous region. A circle is built and extruded.

15. Now right click on Geometry1 located below the definitions in the model builder window. Select 'Cone'. Edit the radius, height and semi-angle field. In the position window edit z such that it lies immediately above the hold-up region. Refer Picture below.

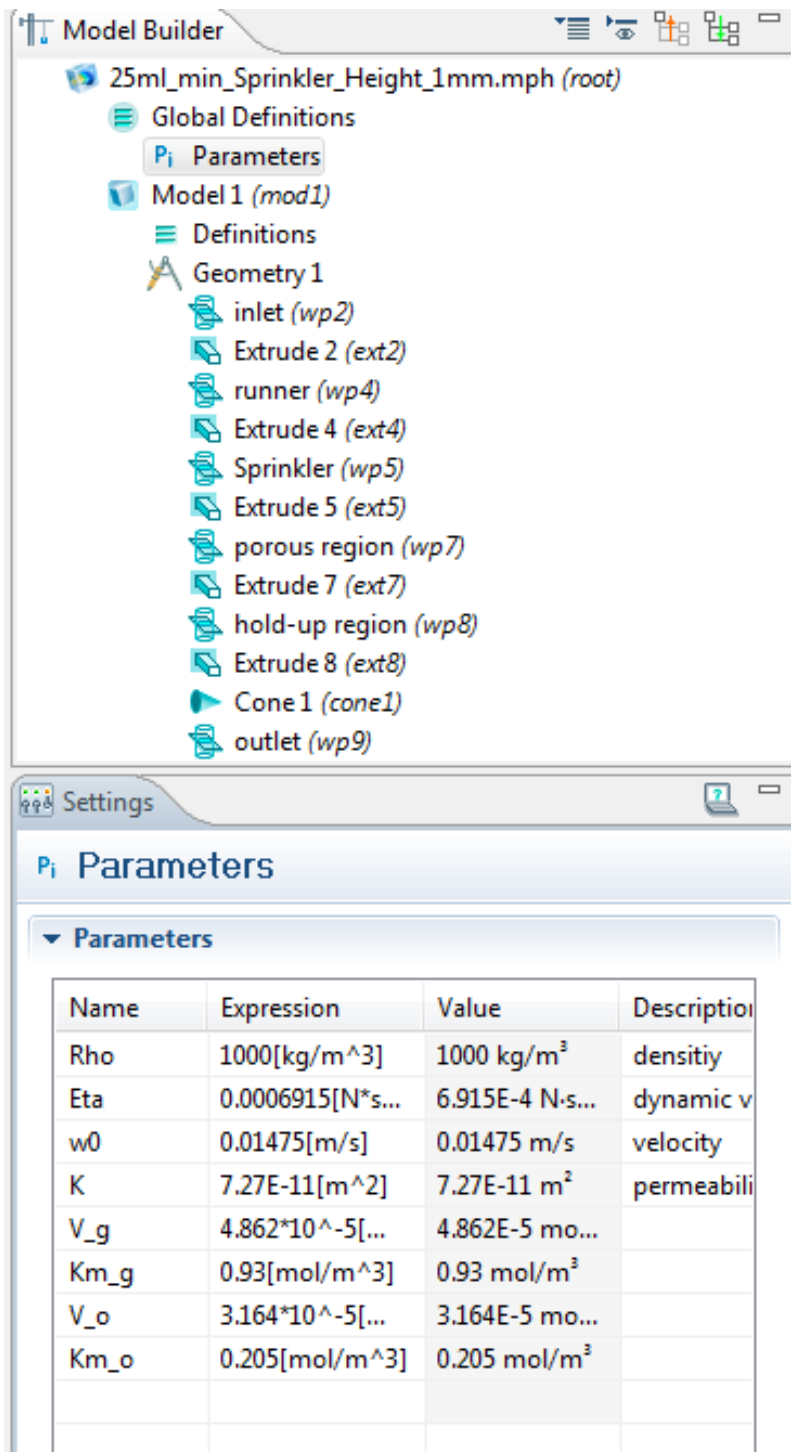


16. Create one more work plane and rename as outlet with z- coordinate immediately above the cone. Build a circle and extrude the work plane.

17. The geometry built is shown below:



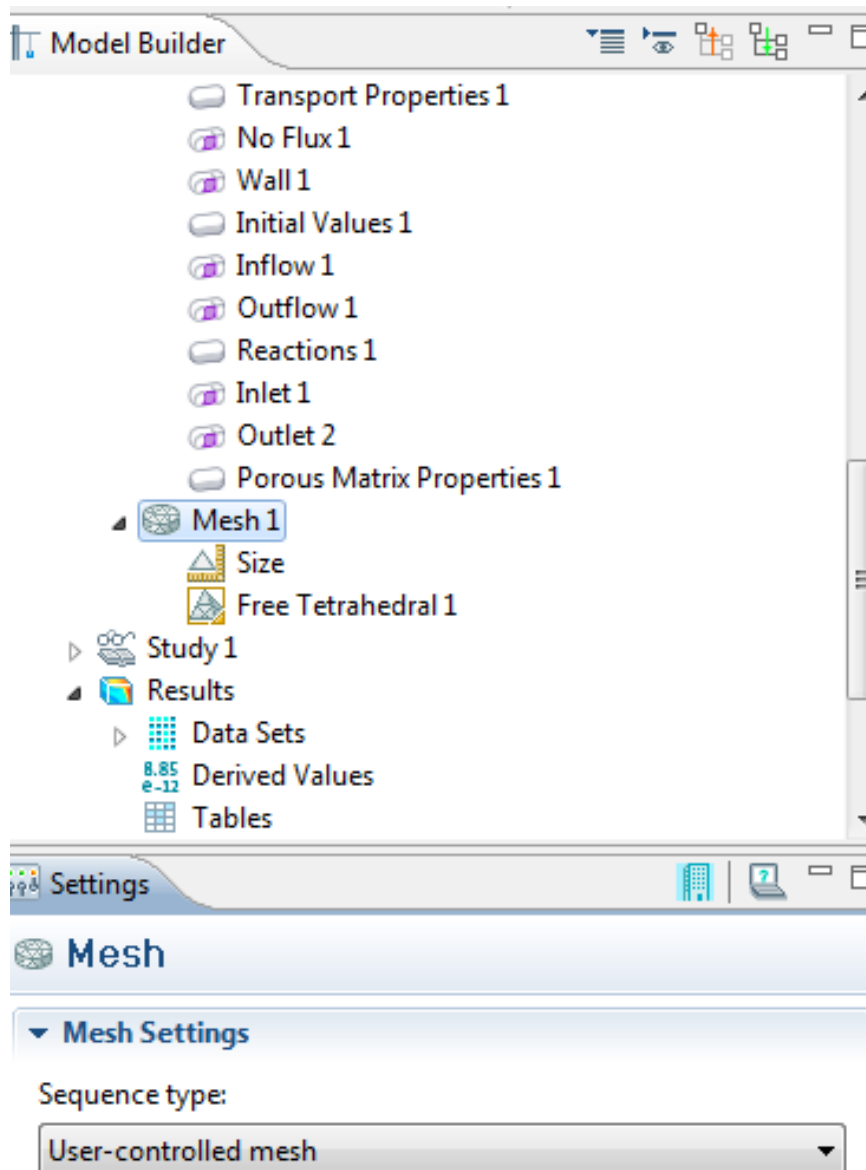
18. Next step is entering the constants and this is done by right clicking on the Global definitions in the model builder window and choosing parameters. Then the required parameter with the variable name, expression, value and description can be typed.



19. The next step is inserting the boundary conditions for the governing equations. Right click on the Reacting Flow, Dilutes Species in the model builder window and select inflow and outflow from the species transport field. Select Inlet and Outlet from the fluid flow field. Select reactions from the Species transport field. Also select the porous matrix properties field. After selecting these fields its necessary to select the domain for each field and any constants for that field. The below is the table showing the field, domain and the constants.

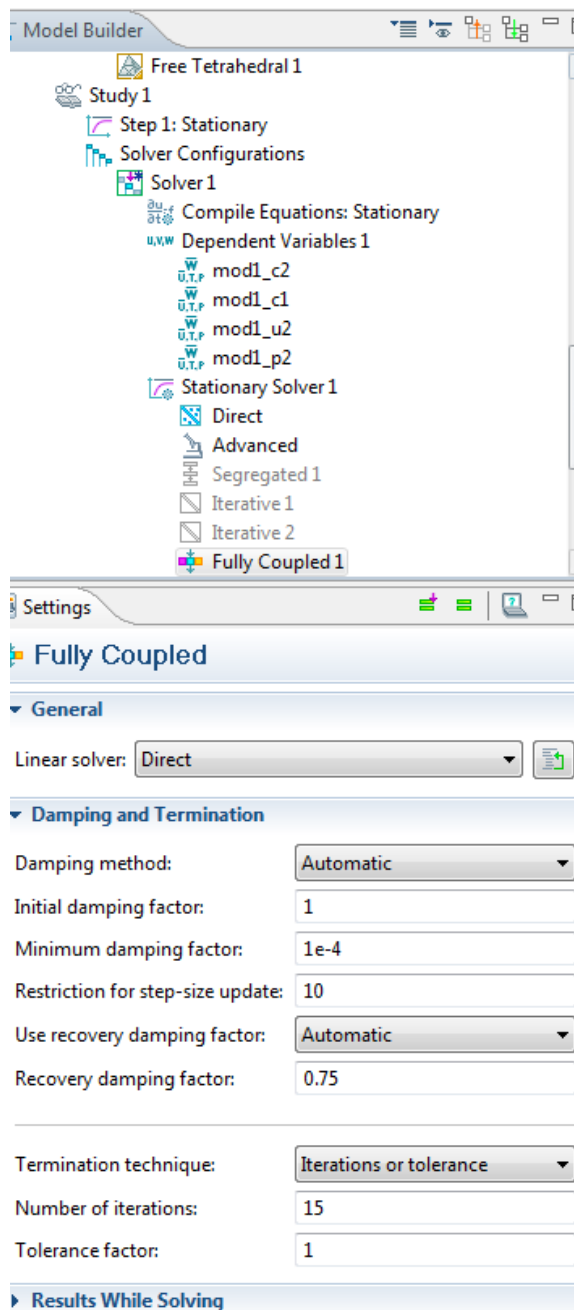
Field	Domain/Boundaries	Constants/Boundary Condition		Values	
Transport Properties	All Domains	Density		Rho(User Defined)	
		Dynamic Viscosity		Eta(User Defined)	
		Diffusion coefficients	D <sub>c1</sub>	1.1937e-9m <sup>2</sup> /s	
			D <sub>c2</sub>	4.8e-9m <sup>2</sup> /s	
No flux	All boundaries	None		Not Applicable	
Wall	All Boundaries	None		Not applicable	
Initial values	All Domains	None		None	
Inflow	Bottom most boundary	C <sub>0,c1</sub>		0.22 mol/m <sup>3</sup>	
		C <sub>0,c2</sub>		5.5 mol/m <sup>3</sup>	
Outflow	Top most boundary	None		None	
Reactions	Porous Region	Reactions R <sub>c1</sub>		-V <sub>o</sub> *c1/(Km <sub>o</sub> +c1)	
	Domain	Reactions R <sub>c2</sub>		-V <sub>g</sub> *c2/(Km <sub>g</sub> +c2)	
Inlet	Bottom most boundary	Velocity	Velocity field,u <sub>0</sub>	0	x
				0	y
				w0	z
Outlet	Top most boundary	Pressure, no viscous stress		0 Pa	
Porous Matrix Properties	Porous Region	Porosity		0.77(User Defined)	
	Domain	Permeability		K(User Defined)	

20. This step explains the meshing portion of the simulation. The sequence type is selected as User-Controlled mesh. The fields below the mesh should be only one size and one free tetrahedral as shown below. In the size field the element size is calibrated for should be selected as General physics and in the free tetrahedral field the domain selection geometric entity level should be selected as Entire geometry.

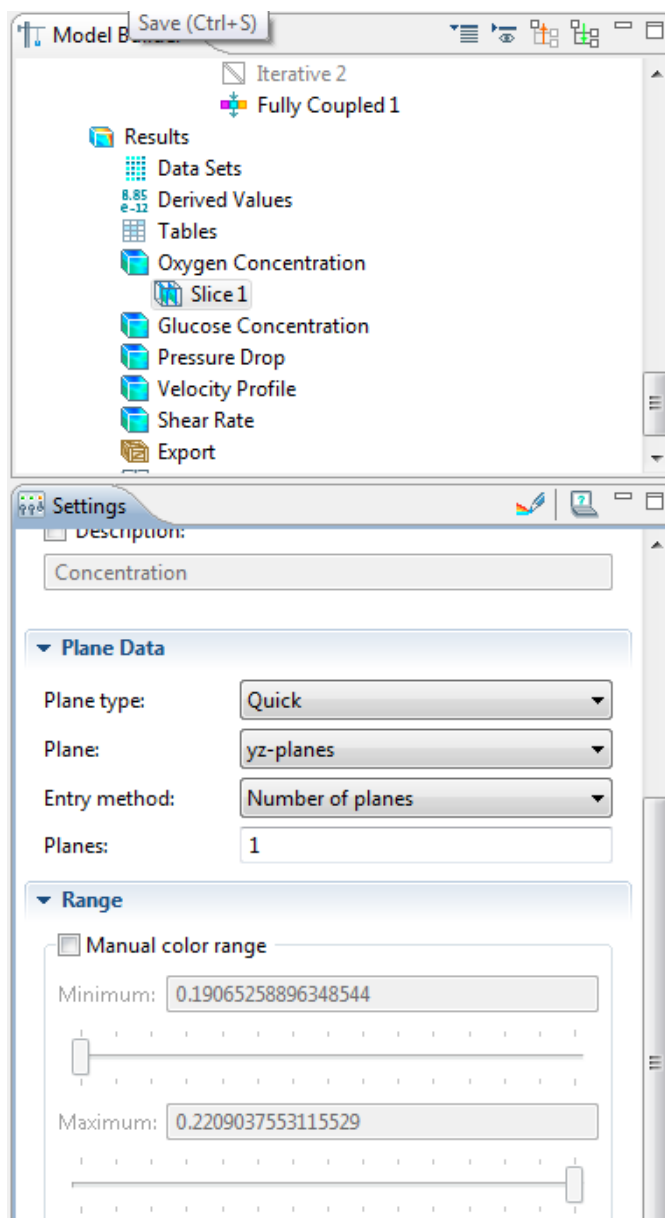




21. Next is setting up the solver. Click in the study1 option in the model builder window to expand and expand the solver configurations and then the solver1. Then expand the stationary solver 1 and then disable the iterative and segregated option. Then click on Fully coupled 1 option and in the settings window damping and termination can be edited. Then compute button is selected to run the simulation.



22. This step explains generating results after running the simulations. Right Click on the Results option in the model builder window and select the 3D plot group and rename it. Then by right clicking the renamed 3D plot group its possible to select a slice plot. The slice plot expressions are modified by clicking on the insert expression option field in the expressions section of the slice window. The units and the plane data can be edited. Also the range has to be edited sometimes.



## APPENDIX B

### Experimental Observations

**Table B.1.Experimental pressure drop without bioreactor**

Flow rate (mL/min)	Pressure Drop(Pa)			Normalized Pressure Drop(Pa)			Average Pressure Drop(Pa)
	Set 1	Set 2	Set 3	Set 1	Set 2	Set 3	
0	676.73	683.16	681.87	0	0	0	0
5	747.47	749.61	749.18	70.74	57.45	67.31	65.2
10	812.63	811.35	806.20	135.91	128.19	124.33	129.5
15	861.10	859.37	858.94	184.35	176.21	177.07	179.2
20	936.97	939.97	938.25	260.24	256.81	256.38	257.8
25	995.27	999.99	1002.56	318.55	316.83	320.69	318.7

**Table B.2. Experimental pressure drop across bioreactor without scaffold**

Flow rate (mL/min)	Pressure Drop(Pa)			Normalized Pressure Drop(Pa)			Average Pressure Drop(Pa)
	Set 1	Set 2	Set 3	Set 1	Set 2	Set 3	
0	-1247.41	-1247.41	-1247.41	0	0	0	0
5	-1176.05	-1180.43	-1179.59	71.36	66.98	67.82	68.7
10	-1110.67	-1118.35	-1122.22	136.75	129.06	125.19	130.3
15	-1061.58	-1069.75	-1068.94	185.83	177.66	178.48	180.7
20	-984.91	-988.31	-988.79	262.50	259.10	258.62	260.1
25	-925.94	-927.72	-923.91	321.48	319.69	323.50	321.6

**Table B.3. Experimental pressure drop across bioreactor with scaffold**

Flow rate (mL/min)	Pressure Drop(Pa)			Normalized Pressure Drop(Pa)			Average Pressure Drop(Pa)
	Set 1	Set 2	Set 3	Set 1	Set 2	Set 3	
0	-1247.41	-1247.41	-732.94	0	0	0	0
5	-1170.50	-1174.76	-659.13	76.91	72.65	73.81	74.46
10	-1098.21	-1105.62	-595.21	149.21	141.79	137.73	142.91
15	-1041.86	-1050.60	-534.97	205.55	196.81	197.96	200.11
20	-958.87	-962.80	-448.46	288.54	284.61	284.48	285.87
25	-890.47	-892.08	-373.45	356.95	355.33	359.49	357.26

**Table B.4 Simulation vs. Experiment pressure drop**

Flow rate (mL/min)	Pressure drop(Pa) w/o scaffold			Pressure drop(Pa) with scaffold		
	Experiment	Std.Deviation	Simulation	Experiment	Std.Deviation	Simulation
0	0	0	0	0	0	0
5	0.5	0.06	0.26	6.3	0.18	6.2
10	0.8	0.02	0.57	13.4	0.15	12.4
15	1.4	0.04	0.92	20.9	0.3	18.9
20	2.3	0.03	1.32	28	0.25	25.2
25	2.8	0.06	1.76	38.6	0.21	31.7

**Table B.5 Mean residence time of bioreactor without distributor and without scaffold**

Time, t(min)	C(t)/C <sub>0</sub>		E(t)		tE(t)	
	AVG	STD	AVG	STD	AVG	STD
0.13	0.00	0.00	1.37	0.12	0.17	0.02
0.38	0.32	0.02	1.13	0.05	0.42	0.02
0.63	0.53	0.08	0.68	0.05	0.42	0.03
0.88	0.80	0.03	0.37	0.03	0.33	0.03
1.13	0.87	0.04	0.20	0.02	0.23	0.02
1.38	0.90	0.04	0.11	0.01	0.15	0.02
1.63	0.88	0.07	0.06	0.01	0.09	0.01
1.88	0.94	0.02	0.03	0.00	0.05	0.01
2.50	0.91	0.08	0.01	0.00	0.01	0.00
3.50	0.96	0.03	0.00	0.00	0.00	0.00
5.00	0.98	0.01	0.00	0.00	0.00	0.00
7.00	0.97	0.04	0.00	0.00	0.00	0.00
9.00	0.97	0.03	0.00	0.00	0.00	0.00
11.00	0.95	0.04	0.00	0.00	0.00	0.00

**Table B.6 Mean residence time of bioreactor with distributor and without scaffold**

Time, t(min)	C(t)/C <sub>0</sub>		E(t)		tE(t)	
	AVG	STD	AVG	STD	AVG	STD
0.25	0.00	0.00	0.46	0.02	0.11	0.00
0.75	0.32	0.01	0.32	0.01	0.24	0.01
1.25	0.36	0.04	0.24	0.00	0.30	0.00
1.75	0.54	0.04	0.18	0.00	0.32	0.00
2.25	0.62	0.05	0.14	0.00	0.32	0.00
2.75	0.73	0.03	0.11	0.00	0.31	0.01
3.25	0.75	0.01	0.09	0.00	0.29	0.01
3.75	0.77	0.04	0.07	0.00	0.26	0.01
4.25	0.85	0.04	0.06	0.00	0.24	0.01
4.75	0.84	0.01	0.04	0.00	0.21	0.01
5.25	0.89	0.01	0.03	0.00	0.18	0.01
5.75	0.88	0.03	0.03	0.00	0.16	0.01
6.25	0.95	0.02	0.02	0.00	0.14	0.01
6.75	0.97	0.02	0.02	0.00	0.12	0.01
7.25	0.97	0.03	0.01	0.00	0.10	0.01
7.75	0.94	0.02	0.01	0.00	0.09	0.01
8.50	0.96	0.06	0.01	0.00	0.07	0.01
9.50	0.95	0.06	0.01	0.00	0.05	0.01
10.50	0.96	0.09	0.00	0.00	0.03	0.01
11.50	0.99	0.07	0.00	0.00	0.02	0.00



**Table B.7 Mean residence time of bioreactor with distributor and with scaffold**

Time, t(min)	C(t)/C <sub>0</sub>		E(t)		tE(t)	
	AVG	STD	AVG	STD	AVG	STD
0.08	0.00	0.00	0.95	0.04	0.08	0.00
0.25	0.36	0.05	0.47	0.02	0.12	0.01
0.42	0.40	0.09	0.33	0.03	0.14	0.01
0.58	0.39	0.06	0.26	0.03	0.15	0.02
0.75	0.40	0.06	0.22	0.02	0.16	0.02
0.92	0.44	0.08	0.19	0.02	0.17	0.02
1.08	0.46	0.05	0.16	0.02	0.18	0.02
1.25	0.61	0.01	0.15	0.02	0.18	0.02
1.42	0.66	0.08	0.13	0.02	0.18	0.02
1.58	0.60	0.03	0.12	0.02	0.19	0.02
1.75	0.57	0.06	0.11	0.01	0.19	0.02
1.92	0.67	0.08	0.10	0.01	0.19	0.02
2.08	0.70	0.16	0.09	0.01	0.19	0.02
2.25	0.67	0.04	0.08	0.01	0.19	0.02
2.42	0.67	0.15	0.08	0.01	0.19	0.02
2.58	0.66	0.04	0.07	0.01	0.19	0.02
2.75	0.65	0.02	0.07	0.01	0.19	0.02
2.92	0.78	0.02	0.06	0.01	0.19	0.02
3.50	0.81	0.03	0.05	0.00	0.18	0.01

## VITA

Prasana Raja Bhaskar

Candidate for the Degree of

Master of Science

Thesis: DESIGN OF AN AXIAL FLOW BIOREACTOR FOR TISSUE  
REGENERATION

Major Field: Chemical Engineering

Biographical:

Education:

Completed the requirements for the Master of Science in Chemical Engineering at Oklahoma State University, Stillwater, Oklahoma in May, 2012.

Completed the requirements for the Bachelor of Engineering in Chemical Engineering and Master of Science in Chemistry at BITS-Pilani, Goa, India in June, 2009.

Experience:

Research and Teaching Assistant, Oklahoma State University, Stillwater, OK.

Professional Memberships:

Chemical Engineering Graduate Student Association

Name: Prasana Raja Bhaskar

Date of Degree: May, 2012

Institution: Oklahoma State University

Location: Stillwater, Oklahoma

Title of Study: DESIGN OF AN AXIAL FLOW BIOREACTOR FOR TISSUE  
REGENERATION

Pages in Study: 91

Candidate for the Degree of Master of Science

Major Field: Chemical Engineering

Scope and Method of Study: Modeling of bioreactors using Computational Fluid Dynamics (CFD) tools have been adapted for several bioreactor configurations such as flow-through, parallel-flow, and rotary. In this study, modeling was mainly performed to analyze the hydrodynamic characteristics, such as shear stress, and pressure drop, and nutrient distribution. The axial flow bioreactor configuration offer several advantages, such as convection-driven nutrient distribution and ability to operate at high flow rates. Hence, this configuration was selected for simulation studies. The geometry of the bioreactor was optimized using COMSOL 4.2 to ensure uniform shear stress and nutrient distribution throughout scaffold. The bioreactor was fabricated in-house for experimental studies. Experimental validation of simulation results were done by measuring pressure drop across the bioreactor and analyzing residence time distribution (RTD) in the bioreactor.

Findings and Conclusions: The hold-up volume of the bioreactor (scaled up) was minimized by increasing the semi-angle of the cone. However, increasing the semi-angle reduced the distribution of nutrients in the outer regions of the scaffold. Uniform nutrient distribution was achieved by incorporating a distribution system at the entrance of the bioreactor. The simulation results showed increase in pressure drop across the bioreactor with increased fluid flow rate and decreased scaffold pore size. Changing the inlet or outlet diameter of the bioreactor had little to no effect on hydrodynamic characteristics or nutrient distribution. The bioreactor configuration with minimum hold-up volume, uniform nutrient and shear stress distribution was selected for experimentation. Experimental measurement of pressure drop across the bioreactor without the scaffold showed good agreement with the simulation results. However, experimental pressure drop across the bioreactor with scaffold showed deviation from simulation results. This was attributed to the skinny layer on top of the scaffold. The residence time distribution experiments suggested a decrease in the dead volume of the bioreactor with the addition of the distribution system. Comparison of nutrient distribution in simulations with experimental RTD showed possible dead zones. Future studies should focus on modifying the distributor system to minimize dead volumes. Cell culture experiments must be conducted on the bioreactor to evaluate the effectiveness of the bioreactor configuration.

ADVISER'S APPROVAL: **Dr. Sundar V. Madihally**

---